-Title: Elevation gradients shape morphology and acoustic phenotype across isolated songbird populations

-Authors: Javier Oñate-Casado[1,2*], Juan Carlos Illera[3], Tereza Petrusková[2], Adam Petrusek[2], Henrik Brumm[1]

*Correspondence: javiatocha@gmail.com

[1] Animal Communication & Urban Ecology Group, Max Planck Institute for Biological Intelligence, 82319 Seewiesen, Germany

[2] Department of Ecology, Faculty of Science, Charles University, Viničná 7, 12843, Prague, Czechia

[3] Biodiversity Research Institute (CSIC-Oviedo University-Principality of Asturias), c/Gonzalo Gutiérrez Quirós, S/N, 33600, Mieres, Asturias, Spain

ABSTRACT

Elevational gradients provide natural experiments for examining how environmental variation shapes animal phenotypes. In birds, geographic variation in body size may also influence song frequency because vocal production is constrained by morphology. We tested whether elevation and temperature are associated with coordinated variation in morphology and song frequency in Berthelot's pipit (*Anthus berthelotii*), a songbird endemic to Macaronesia. We measured song characteristics and male morphology across elevational and thermal gradients on three islands: Tenerife, La Palma, and Madeira. We tested relationships between environmental conditions, song frequency, a composite body-size index, and individual morphological traits using linear mixed-effects models. Song peak frequency decreased by approximately 249 Hz per 1000 m increase in elevation and by 570 Hz per 10 °C decrease in annual mean temperature. These relationships were consistent among islands. Body size showed similar elevational and thermal

responses: the multivariate body-size score increased by 0.316 units per 1000 m of elevation, and by 0.690 units per 10 °C decrease in temperature. Higher, colder environments were therefore associated with both larger males and lower-frequency songs. This parallel variation is consistent with predictions from Bergmann's rule and suggests that environmental effects on morphology translate into geographic variation in song frequency. Thus, environmental gradients can structure multiple, functionally connected phenotypic traits within a species. By linking elevational variation in climate with coordinated changes in morphology and song across geographically isolated populations, this study shows how ecological variation can propagate across different levels of phenotype and thereby contribute to geographic variation in animal behavior.

Keywords: *acoustic variation, animal communication, Bergmann's rule; bird song; body size; environmental variation; geographic variation; island populations; song frequency*

INTRODUCTION

Elevational gradients provide powerful natural experiments for examining how environmental variation is associated with geographic variation in animal phenotypes (Körner, 2007). In mountainous landscapes, elevation is typically accompanied by pronounced changes in temperature and atmospheric conditions, as well as by regional variation in precipitation, vegetation, and resource availability, often over relatively short geographic distances (Alice Boyle et al., 2016; Laiolo & Obeso, 2017). Animals inhabiting these gradients may therefore experience substantial variation in both the abiotic and biotic factors that shape their morphology, physiology, and behavior. In particular, temperature generally declines predictably with elevation, making mountain gradients useful for evaluating predictions about body-size variation in relation to thermal environment (Körner, 2007; Laiolo & Obeso, 2017).

A prominent framework concerning geographic variation in body size is Bergmann's rule, which describes the tendency for endothermic animals to be larger in colder environments than in warmer ones (Bergmann, 1848). Its classic explanation is thermoregulatory: for organisms of similar shape, larger bodies have a lower surface-area-to-volume ratio, therefore lose heat more slowly. Smaller bodies, on the other hand, facilitate heat dissipation in warmer climates. Accordingly, larger individuals are expected to occur at higher latitudes because average temperatures typically drop towards the poles. In birds and mammals, a substantial body of evidence supports Bergmann's rule at both interspecific and intraspecific levels (Ashton, 2002; Meiri & Dayan, 2003; Olson et al., 2009; Clauss et al., 2013; Romano et al., 2021). However, global analyses also show that, across taxa and geographic scales, variation in latitude or temperature accounts for only a modest proportion of variation in body size, emphasizing that

Bergmann's rule reflects a broad statistical tendency rather than a universal response (Gohli & Voje, 2016; Riemer et al., 2018).

Elevational gradients provide an additional context in which to examine Bergmann-like patterns, but there is inconsistent evidence that birds become larger at higher elevations. Some montane bird species exhibit positive correlations between body size and elevation, as observed in Andean passerines (Blackburn & Ruggiero, 2001) and, more recently, in house sparrows (*Passer domesticus*) sampled across a wide range of elevations in the Himalayas (Bala et al., 2024). However, the detected relationship in the Andean birds was only weak (Blackburn & Ruggiero, 2001), and intraspecific studies found little or no relationship between elevation and body size (Freeman, 2017) or even negative ones (Youngflesh et al., 2022).

This suggests that the thermal benefits of increased body size may be counteracted by other ecological pressures at high elevations. Furthermore, environmental effects are not necessarily expressed uniformly across morphological traits. Different measures of body size may differ in their functional relationships with temperature and other selective pressures, such as the demands from flight or locomotion (Youngflesh et al., 2022; Yang et al., 2025), and food availability (Cresswell, 1998; Cox et al., 2011). Thus, evaluating elevational variation using multivariate measures of body size alongside individual morphological traits may provide a more informative assessment of how birds respond to environmental gradients than any single measure of size.

Geographic variation in body size may also affect traits that are constrained by morphology. In birds, for example, song frequency is strongly associated with body size, with larger species tending to produce lower-frequency vocalizations (Wallschläger, 1980; Mikula et al., 2021), a relationship that has also been observed within species (e.g. Linhart & Fuchs, 2015; Brumm & Goymann, 2017). This connection is thought to arise from the scaling of the syrinx and the vocal

tract with body dimensions, placing constraints on the frequencies that birds can efficiently produce (Ryan & Brenowitz, 1985; Podos, 2001; Suthers & Zollinger, 2008). Consequently, the same environmental factors that influence body size could indirectly generate geographic variation in song frequency. Such indirect effects are particularly interesting from a biogeographical perspective because they imply that environmental gradients may structure communication signals not only through direct selection on acoustic traits, but also through their effects on morphology. If body size increases in colder environments as predicted by Bergmann's rule, a corresponding decrease in song frequency could emerge as a correlated consequence of morphological variation.

Recent studies provide initial evidence for such a link between elevation, body size, and avian song. In African tinkerbirds (*Pogoniulus* spp.), song frequency decreased with elevation and latitude, both across taxa and within individual taxa, in parallel with geographic variation in body size, leading to the suggestion that large-scale variation in song pitch may partly arise as a consequence of Bergmann-like body-size variation rather than solely through direct adaptation to local acoustic environments (Sebastianelli et al., 2022). Similarly, African fiery-necked nightjars (*Caprimulgus pectoralis*) sing lower-frequency songs at higher elevations, although song frequency did not vary with latitude in this species (Comin & Brumm, 2025). Across the family of honeyeaters (Meliphagidae), body size strongly constrained song frequency, with larger species producing lower-frequency songs, while environmental variation also contributed to differences in acoustic traits (Hay et al., 2024). Together, these studies suggest that environmental variation in morphology may propagate into geographically structured variation in acoustic signals. However, direct tests of this idea within species and across fine-scale elevational gradients remain limited. In particular, we are not aware of any study that has tested

whether body-size variation consistent with Bergmann's rule is accompanied by corresponding changes in song frequency along the same gradients.

We examined this topic in Berthelot's pipit (*Anthus berthelotii*), a species particularly well-suited to examining geographic variation in song across environmental gradients. This sedentary oscine passerine is endemic to Macaronesia and occurs in isolated island populations in three oceanic archipelagos: the Canaries, Madeira, and Selvagen islands (Illera et al., 2007). Oceanic islands are widely recognized as natural laboratories for studying ecological and evolutionary processes because they constitute discrete and replicated systems in which ocean barriers can restrict dispersal and gene flow, while environmental conditions vary among them (Warren et al., 2015; Whittaker et al., 2017). In Berthelot's pipit, this isolation is reflected by limited gene flow between populations from different archipelagos, as well as between islands within the same archipelago (Illera et al., 2007; Spurgin et al., 2014; Armstrong et al., 2018; Martin et al., 2021). Previous research showed that territorial males have individually distinct songs, while a weak geographic signal remains detectable across islands and archipelagos (Oñate-Casado et al., 2026). Across some Macaronesian islands, Berthelot's pipits also occur over large elevational ranges, spanning substantial climatic variation from sea level to alpine habitats.

Here, we tested whether song frequency in Berthelot's pipit varies along elevational and thermal gradients across the islands of Tenerife, La Palma, and Madeira, and whether these acoustic patterns are accompanied by parallel variation in male morphology. We selected these three island populations because they span broad elevational and climatic gradients (Prada et al., 2009; Gonzalez-Quevedo et al., 2014; Steinbauer et al., 2017), providing substantial environmental variation within and among islands. We predicted that song frequency would decrease with elevation and increase with temperature. If this acoustic pattern is driven by morphological

variation consistent with Bergmann's rule, males from higher, colder locations should show larger overall body size, together with individual morphological traits showing corresponding responses. We also tested whether these acoustic and morphological relationships were consistent among islands. Together, these analyses allowed us to test whether a shared elevational-thermal gradient is associated with coordinated variation in morphology and song frequency across isolated island populations, as expected under a Bergmann-related explanation for geographic variation in song frequency.

METHODS

Study system and sampling

The Berthelot's pipit is a sedentary passerine endemic to the Macaronesian archipelagos, where it occurs in various open habitats, such as rocky areas in plains, hillsides with sparse vegetation, clearings in wooded areas and scrubby slopes, from sea level to alpine habitats further inland, reaching elevations above 2500 m on Tenerife (Illera, 2007; Illera et al., 2007). The species is territorial and socially monogamous, and males sing intensively for several weeks at the onset of the breeding season (closely linked to rainfall), typically from late January to late February, although breeding and singing begin later at the highest elevations (Martín & Lorenzo, 2001; Oñate-Casado et al., 2026). Their songs are individually distinct, allowing different singing males to be distinguished acoustically without the need to capture and mark individuals before recording (Oñate-Casado et al., 2026).

We focused on three island populations: Tenerife and La Palma in the Canary Islands, and Madeira in the Madeira archipelago. Together, these populations encompass broad elevational and climatic variation (Figure 1; Table 1). Acoustic recordings were obtained during a single breeding season on each island, in mid- to late February, following the sampling design

described by Oñate-Casado et al., (2026). Recordings were obtained in Madeira in 2020 and in Tenerife and La Palma in 2021. The acoustic dataset included 254 males (Tenerife: n = 139; La Palma: n=77; Madeira: n=38).

Morphological data were collected between 2005 and 2020 and comprised 126 males (Tenerife: n = 74; La Palma: n = 29; Madeira: n = 23). Birds were captured from late January to late April on La Palma, in mid-September on Madeira, and from mid-February to late May on Tenerife. Most of the measurements were derived from field studies described by Illera et al., (2007) . In these samples, birds were individually ringed and measured following standardized field procedures. The dataset was then supplemented by further sampling carried out by J.C. Illera up to 2020 (see Table 1 for details).

Song recording and acoustic measurements

The song recording and acoustic analysis are described in detail in Oñate-Casado et al., (2026). In brief, territorial singing males were recorded using Sennheiser ME-67 directional microphones connected to Marantz PMD 661 digital recorders. All acoustic measurements were obtained from males producing repeated, structurally consistent territorial songs during the breeding season.

For each male, a high-quality rendition of its representative song type was selected for acoustic measurements (i.e. each individual was represented by a single song), as males repeat their song types with high-individual consistency (Oñate-Casado et al., 2023) and this seems to be temporally stable (JO-C, unpubl. Data). Recordings were first inspected in Avisoft-SASLab Lite 5 (Specht, 2007) and then processed in Luscinia v.2.24.09.12.02, a software for bioacoustic archiving, measurement and analysis (Lachlan, 2024). Acoustic measurements were obtained at both the whole-song level and the level of the individual elements composing each song. We

defined an element as a discrete unit of continuous sound separated from other elements by silence, and a song as the complete sequence of elements contained within a single rendition. Frequency measurements were then extracted for both the complete song and its individual elements using the same spectrogram and measurement settings as in Oñate-Casado et al., (2026).

For this study, we used two frequency-based measures: song peak frequency, calculated across the entire song, and mean element peak frequency, calculated as the average peak frequency across all elements within that song. Song peak frequency therefore reflects the dominant frequency of the whole song, whereas mean element peak frequency reflects the average dominant frequency of its individual elements. Song peak frequency was treated as the primary acoustic response, whereas mean element peak frequency provided a complementary measure of the overall spectral position of the song elements. Spectrograms of songs with the lowest and highest song peak frequency on each island are shown in Fig. S2.

Morphological measurements

Morphological data included four traits: wing length, head length, tarsus length, and body mass; see Illera et al., (2007) for details. The dataset was restricted to individuals confirmed as males by molecular sexing (Illera et al., 2007) to exclude potential sex-related variation along the environmental gradient.

For tarsus length, measurements of the left and right tarsi were averaged when both were available to obtain a single value per individual. When only one measurement was available, it was used directly as the individual's tarsus length. The resulting morphology dataset contained 126 males with wing-length data, while head length, tarsus length and body mass were each available for 125 males.

Environmental variables

Environmental variables were assigned to the geographic coordinates associated with each acoustic and morphological observation using R version 4.5.2 (R Core Team, 2025). Elevation data were obtained from the SRTM 30 m digital elevation model through the OpenTopoData API using the *httr2* package (Wickham, 2021), with bilinear interpolation applied at each sampling coordinate. Climatic variables were obtained from WorldClim bioclimatic layers at 2.5 arc-minute resolution using the *geodata* R package (Hijmans, 2021) and extracted at sampling coordinates using the *terra* R package (Hijmans et al., 2020) for spatial data processing. These included annual mean temperature (BIO1) and minimum temperature of the coldest month (BIO6). Direct WorldClim extraction returned missing values for three acoustic records located very close to the coast, likely because their coordinates fell on land-ocean raster boundaries; for these records, climate values were estimated by bilinear interpolation from neighboring raster cells.

Elevation and temperature were included to characterize the elevational-thermal gradient along which we evaluated variation in both song frequency and morphology. The morphology data were used to assess whether variation in song frequency along this gradient was accompanied by morphological changes consistent with the predictions from Bergmann's rule. Individual-level metadata, environmental variables, and acoustic measurements for all males included in the acoustic analyses are provided in Table S1, while corresponding metadata, environmental variables, and morphological measurements for all males included in the morphological analyses are provided in Table S2.

Statistical analysis

All statistical analyses were conducted in R version 4.5.2 (R Core Team, 2025). Figures were produced using the *ggplot2* package (Wickham, 2016). The spatial data for the sampling map was processed with the *sf* and *terra* packages (Pebesma, 2016; Hijmans et al., 2020). Because the acoustic and morphological datasets were obtained from different individuals and in different years, they were analyzed independently. We therefore evaluated whether acoustic and morphological traits showed parallel relationships with the same broad environmental gradients, rather than testing within-individual associations between morphology and song.

We used linear mixed-effects models to test whether acoustic and morphological traits varied along environmental gradients while accounting for differences among island populations and for individuals sampled within the same locality (acoustic data) or sampling location (morphology data). Models were fitted using the *lme4* package (Bates et al., 2003), with the *lmerTest* package (Kuznetsova et al., 2013) used to obtain P-values for fixed-effect estimates. We compared a series of nested models, in which environmental predictors and their interactions with island population were added sequentially, using likelihood-ratio tests fitted by maximum likelihood. This allowed us to test first whether including an environmental gradient improved model fit and then whether the strength of that relationship differed among islands. Where an interaction indicated that the environmental relationship differed among island populations, the *emmeans* package (Lenth & Piaskowski, 2017) was used to estimate and compare the relationship among corresponding populations.

Environmental covariation

Prior to fitting the environmental models, we examined the pairwise Pearson correlations between the environmental predictors to evaluate the degree to which they represented

independent or overlapping environmental gradients. Elevation, annual mean temperature (BIO1), and minimum temperature of the coldest month (BIO6) were strongly correlated, and BIO1 and BIO6 provided very similar descriptions of thermal variation (see the Results section for details). We therefore retained BIO1 as the primary temperature variable and excluded BIO6 from formal models to avoid redundant analyses. Elevation and BIO1 were analyzed in separate models rather than simultaneously because their strong covariation would make their independent effects difficult to distinguish. Together, elevation and BIO1 were treated as alternative descriptors of the same broad elevational-thermal gradient.

Acoustic models

Song peak frequency and mean element peak frequency were analyzed separately using linear mixed-effects models. Because the two peak frequency responses were derived from the same song, they were not considered statistically independent and were thus interpreted as complementary measures rather than independent tests of the same pattern. All acoustic models included recording locality within island population as a random intercept to account for multiple males recorded within the same locality. Given the opportunistic nature of sampling (i.e. recording as many males as possible across different locations within each island), localities were defined as named sampling areas corresponding to spatial clusters of birds encountered during fieldwork.

For each acoustic response and each environmental predictor, we fitted three nested models. The baseline model included island population as its only fixed effect, allowing mean acoustic frequency to differ among islands but assuming no environmental relationship. A second model added the environmental predictor and tested whether acoustic frequency varied along that gradient after accounting for average differences among populations. A third model added the

interaction between population and the environmental predictor to test whether the strength of the environmental relationship differed among islands. The baseline and environmental models were compared to assess support for an overall environmental association, whereas the environmental and interaction models were compared to assess whether that association varied among populations.

Elevation and annual mean temperature (BIO1) were each analyzed in separate model sets. This allowed us to evaluate each environmental relationship independently while avoiding the inclusion of strongly correlated predictors in the same model.

Multivariate morphology

We performed a principal component analysis (PCA) using wing length, head length, tarsus length, and body mass to create a composite measure of morphological variation. The analysis was restricted to males with complete measurements for all four traits. Because the variables were measured on different scales, all traits were centered and standardized before PCA using the *prcomp* function in R.

The first principal component (PC1), capturing 55.4% of variation of morphological data, was retained as the main multivariate morphology axis because all four traits contributed positively and relatively evenly to it, so higher PC1 scores represented individuals with generally larger morphological measurements. We then tested whether PC1 varied with the two environmental predictors that define the core elevational-thermal gradient considered in this study: elevation and annual mean temperature (BIO1). These predictors were analyzed separately using the same three-model hierarchy described above: a baseline model containing island population, a second model adding the environmental predictor, and a third model including the interaction between population and the environmental predictor. To account for multiple individuals sampled at the

same location, we included sampling location as a random intercept, defining each location by a unique pair of recorded latitude and longitude coordinates.

Trait-specific morphology

In addition to the composite morphology score, we also analyzed wing length, head length, tarsus length, and body mass separately to determine whether individual morphological traits showed consistent responses along the same elevational-thermal gradient. Elevation and annual mean temperature (BIO1) were analyzed separately for each trait using the same three-step nested mixed-model structure described above (baseline, environmental and interaction models), with island population included as a fixed effect and sampling location as a random intercept.

Model assessment and sensitivity analyses

Model assumptions and the overall fit of the mixed-effects models were assessed using standard residual diagnostics (checking linearity, homogeneity of variance and normality). When the variance associated with a random effect was estimated at or near zero, we fitted the equivalent ordinary linear model to check whether the main results depended on including that random effect. For the acoustic dataset, several males were sampled within the same localities, so we also repeated the main environmental analyses using locality-level mean values. This provided a more conservative test of whether the same relationships were recovered when each locality, rather than each individual bird, was treated as an independent sampling unit.

RESULTS

Environmental structure

Pearson correlations showed that environmental conditions were strongly structured along elevation. In the acoustic dataset, elevation was strongly negatively correlated with both the

annual mean temperature (BIO1; r = -0.958) and the minimum temperature of the coldest month (BIO6; r = -0.962). Furthermore, BIO1 and BIO6 were highly correlated with each other (r =0.955). The same pattern was observed in the morphology dataset, with a strong negative correlation found between elevation and both the annual mean temperature (BIO1; r = -0.980) and minimum temperature of the coldest month (BIO6; r = -0.974). Because BIO1 and BIO6 closely mirrored elevation, BIO1 was retained as the principal thermal predictor in subsequent analyses.

Acoustic variation along the elevational-thermal gradient

Linear mixed-effects models showed that both acoustic frequency measures varied consistently along the elevational-thermal gradient (Fig. 2; Table S3). Song peak frequency decreased on average by approximately 249 Hz per 1000 m elevation ($\chi^2 = 8.35$, df = 1, P = 0.004) and by approximately 57 Hz per 1 °C decrease in annual mean temperature ($\chi^2 = 10.11$, df = 1, P = 0.001). There was no evidence that the strength of either relationship differed between islands (elevation: $\chi^2 = 1.89$, df = 2, P = 0.390; temperature: $\chi^2 = 1.96$, df = 2, P = 0.376).

Mean element peak frequency showed the same overall response, decreasing by approximately 134 Hz per 1000 m elevation ($\chi^2 = 7.70$), df = 1, P = 0.006) and by approximately 26 Hz per 1 °C decrease in annual mean temperature ($\chi^2 = 6.22$, df = 1, P = 0.013). Again, there was no evidence that the strength of the environmental relationship differed between populations (elevation: $\chi^2 = 2.46$, df = 2, P = 0.293; temperature: $\chi^2 = 1.50$, df = 2, P = 0.473).

Locality-level sensitivity analyses produced the same qualitative conclusions as the individual-level mixed-effects models, with similar directions and approximate magnitudes of the main environmental relationships (Table S4).

Morphological traits and multivariate body size score

Principal component analysis revealed covariation between wing length, head length, tarsus length, and body mass (Fig. S4). PC1 explained 55.4% of standardized morphological variation, with all four traits contributing positively to this axis (wing = 0.493, head = 0.532, tarsus = 0.440, body mass = 0.529). Higher PC1 scores therefore represented individuals with generally larger values across the measured traits. For simplicity, we refer to PC1 hereafter as the multivariate body-size index.

Linear mixed-effects models showed that the multivariate body-size index also varied along the elevational-thermal gradient (Fig. 3; Table S5). It increased by 0.316 units per 1000 m elevation ($\chi^2 = 6.85$, df = 1, P = 0.009) and decreased by 0.069 units per 1 °C increase in annual mean temperature ($\chi^2 = 6.73$, df = 1, P = 0.010). There was no evidence that either relationship differed between islands (elevation: $\chi^2 = 4.37$, df = 2, P = 0.112); temperature: $\chi^2 = 3.91$, df = 2, P = 0.142).

Trait-specific morphological responses

Trait-specific mixed-effects models showed that environmental relationships were most consistent for wing and head length (Fig. S5; Table S5). Wing length increased by approximately 0.4 mm per 1000 m elevation ($\chi^2 = 5.77$, df = 1, P = 0.016) and decreased by 0.1 mm per 1 °C increase in annual mean temperature ($\chi^2 = 5.69$, df = 1, P = 0.017). Head length showed a similar pattern, increasing by approximately 0.3 mm per 1000 m elevation ($\chi^2 = 16.19$, df = 1, P <0.001) and decreasing by 0.1 mm per 1 °C ($\chi^2 = 15.12$, df = 1, P <0.001). For both traits, island × environment interactions were not statistically supported.

In contrast, tarsus length did not vary with elevation ($\chi^2 = 0.96$, df = 1, P = 0.328) or temperature ($\chi^2 = 0.78$, df = 1, P=0.376). Body mass showed no common association with environmental

gradients across islands (Table S5), but island × environment interactions were supported for both elevation ($\chi^2 = 9.23$, df = 2, P = 0.010) and temperature ($\chi^2 = 7.87$, df = 2, P = 0.020), indicating that body-mass responses differed among islands.

Island-specific slopes showed that this heterogeneity was driven primarily by Madeira (Table S6). In Madeira, body mass increased by 0.7 g per 1000 m elevation (P = 0.024) and decreased by 0.2 g per 1 °C increase in temperature (P = 0.041). In Tenerife, body mass showed no supported change with either elevation (P = 0.827) or temperature (P=0.686), whereas La Palma showed weak trends in the opposite direction to Madeira (elevation: P = 0.068; temperature: P = 0.083). Thus, body mass responded differently between islands, indicating a more island-specific pattern than was observed for the other morphological traits.

For wing length, the sampling-location random-effect variance was estimated as zero in both the elevation and temperature model sets. Equivalent ordinary linear models yielded nearly identical slopes and the same qualitative conclusions as the mixed-effects models.

Overall, the acoustic and morphological analyses showed parallel variation in morphology and song along the elevational-thermal gradient. Higher, colder locations were characterized by lower-frequency songs and higher values of the multivariate body-size index, although responses of some individual morphological traits were not uniform.

DISCUSSION

Our results demonstrate coordinated geographic variation in morphology and song frequency across an elevational gradient in Berthelot's pipit. Males occurring at higher and colder locations were generally larger and produced lower-frequency songs, and these relationships were broadly consistent across Tenerife, La Palma, and Madeira. Both peak frequency and mean element frequency declined with elevation and temperature, while the multivariate body-size index

increased along the same environmental gradient. These findings extend a growing body of work showing that geographic variation in avian vocalizations can be associated with broad-scale environmental gradients and suggest that climatic variation may influence song phenotype partly through its effects on morphology (Sebastianelli et al., 2022; Hay et al., 2024).

Elevational variation in song frequency

The negative relationship between elevation and song frequency is consistent with a growing body of evidence documenting geographic variation in avian song along environmental gradients. Lower-frequency songs at higher elevations have been reported in several species from different avian lineages, including green hylia (Passeriformes; Kirschel et al., 2009), African tinkerbirds (Piciformes; Sebastianelli et al., 2022), and, most recently, fiery-necked nightjars (Caprimulgiformes; Comin & Brumm, 2025). Our results therefore add Berthelot's pipit to a still small set of species spanning several avian orders for which elevational variation in song frequency has been documented within species. The magnitude and direction of the association were also similar for our two different measures of song frequency, suggesting that the pattern is not attributable to variation in a single aspect of the song spectrum.

The emerging comparative picture, however, does not indicate a general effect of elevation on birdsong. For example, Caro et al., (2013) found that grey-breasted wood-wrens (*Henicorhina leucophrys*) produced higher-frequency songs at higher elevations, together with a concurrent elevational reduction in body size. Also, the relationship between song frequency and elevation can differ from that with latitude, as shown by Comin & Brumm (2025) in fiery-necked nightjars. Such contrasting patterns emphasize that elevation itself is unlikely to be a direct and universal selective agent on song frequency. Rather, elevation represents a composite environmental gradient along which temperature, vegetation, atmospheric conditions, resource

availability, community composition and other ecological factors may change simultaneously. The direction of vocal variation will therefore depend on which of these factors most strongly constrains or selects the signal in a particular species.

In Berthelot's pipit, the parallel relationships of song frequency with both elevation and annual mean temperature are consistent with the hypothesis that the thermal environment is a key component of the elevational signal. This interpretation is especially plausible given the simultaneous morphological response documented here. However, other environmental mechanisms remain possible. Elevation can modify habitat structure and sound transmission, and acoustic adaptation theory predicts that signal frequency may evolve in response to the transmission properties of the local environment (Brumm & Naguib, 2009). However, this mechanism may be less plausible in Berthelot's pipit, which occurs predominantly in open habitats with sparse vegetation (Illera, 2007; Illera et al., 2007). Evidence for such effects at broad geographic scales is also mixed. For example, a global analysis of passerines found no support for habitat structure as a major determinant of song frequency after accounting for body size (Mikula et al., 2021), whereas Sebastianelli et al., (2022) found some evidence for effects of vegetation density in African tinkerbirds. Thus, the present results are most appropriately interpreted as evidence for environmentally structured song variation, rather than demonstrating a direct causal effect of temperature on song frequency, with associated variation in body size providing a plausible mediating pathway.

Morphological variation and Bergmann's rule

The morphological results provide a second, complementary component to this interpretation. The increase in body size with elevation and its decrease with temperature are consistent with the predictions from Bergmann's rule, whereby larger-bodied individuals occur in colder

environments (Bergmann, 1848). Such relationships have been documented across birds at both broad geographic scales and within species, although their strength and direction vary among taxa and (Ashton, 2002; Meiri & Dayan, 2003; Olson et al., 2009; Romano et al., 2021). The pattern observed here therefore supports the idea that elevational gradients can reproduce, over relatively short geographic distances, some of the geographic phenotypic structure traditionally examined along latitudinal gradients.

At the same time, our trait-specific analyses reveal substantial heterogeneity in how individual morphological traits responded to the elevational-thermal gradient. Wing and head length increased consistently with elevation and decreased with temperature, whereas tarsus length showed no detectable relationship with either environmental variable. Body mass was more heterogeneous still, increasing with elevation in Madeira but showing no supported relationship in Tenerife and a weak tendency in the opposite direction in La Palma. Thus, the overall increase in the multivariate body-size score appears to reflect coordinated changes in several structural traits rather than a generalized increase in every component of body size.

This pattern is important because morphological traits are subject to multiple and sometimes competing selective pressures. Thermoregulatory advantages of larger size in colder environments may favor increased body dimensions, while flight performance, locomotion, food availability, and energetic constraints may favor different morphological optima for particular traits. Along this line, the increase in head length may partly reflect the broader increase in body size towards colder environments, although its comparatively strong and consistent response suggests that head morphology may not simply scale uniformly with other body dimensions. Interestingly, previous work in Berthelot's pipit identified genetic variation associated specifically with head length, rather than with wing length, tarsus length, body mass or bill

measurements (Martin et al., 2021), suggesting that this trait may have a partly distinct genetic basis. The increase in wing length could similarly reflect the general increase in body size, but may additionally be connected to demands from flight. Indeed, the increase in wing length towards higher elevations is consistent with broader evidence that wing morphology can respond to elevation independently of overall body size (Youngflesh et al., 2022). Likewise, Yang et al., (2025) found that wing size increases globally across bird species with elevation after accounting for body mass, potentially reflecting aerodynamic constraints associated with declining air density at higher elevations. Similarly, it is conceivable that stronger winds at higher elevations may also affect the evolution of wing morphology. The longer wings in Berthelot's pipit may thus reflect not only the increase in body size towards higher, colder environments, but potentially also other elevation-related influences on flight performance.

Previous macroecological studies have found that support for Bergmann's rule varies among traits and taxa, highlighting the importance of considering body size as a multidimensional phenotype rather than relying on a single proxy (Ashton & Feldman, 2003; Romano et al., 2021; Sebastianelli et al., 2022). The stronger and more consistent responses of wing and head length than of tarsus length and body mass in Berthelot's pipit reinforce this point.

Linking morphology and song

The most interesting implication of the parallel environmental responses is that geographic variation in song may emerge as a consequence of environmentally associated morphological variation. Body size is strongly and consistently related to song frequency across birds, with larger birds producing lower-frequency sounds (Wallschläger, 1980; Mikula et al., 2021). This relationship is thought to arise from biomechanical constraints associated with the dimensions of the syrinx and vocal tract, which place limits on the frequencies that can be generated efficiently

(Podos, 2001; Suthers & Zollinger, 2008; Rodríguez et al., 2015). Consequently, an environmental effect on body size can potentially propagate into acoustic phenotype without requiring direct selection on song frequency itself.

Our findings fit this conceptual model particularly well because both higher and colder environments were associated with larger males and lower-frequency songs. A similar correspondence between climatic gradients, body size, and song frequency has been reported at broader spatial scales in African tinkerbirds, where song pitch decreased with elevation and latitude in parallel with increases in body size (Sebastianelli et al., 2022). Across honeyeaters, body size has likewise emerged as an important predictor of song frequency, while temperature and elevation were also associated with aspects of song variation, some of which may reflect underlying environmental effects on morphology (Hay et al., 2024). Our study extends this emerging pattern to an intraspecific elevational system, showing that environmental covariation between morphology and song can occur in several populations of a single island-associated species. Although the notion that body size mediaties the relationship between the environment and song is highly plausible, our data cannot rule out other possible mechanisms, such as direct effects of the acoustic environment, behavioral divergence, or other population-level processes. A more direct test would require demonstrating the link between morphology and song frequency within individuals, followed by investigating whether the temperature effect on song is reduced after accounting for morphology. Such an analysis would provide direct evidence of whether the geographic pattern reflects an environmentally induced morphological constraint on vocal production.

This distinction is important from an evolutionary perspective. If song frequency is constrained by morphology, geographically structured body size could generate predictable geographic

variation in a vocal signal even without local selection acting directly on that signal. Conversely, once such variation exists, song frequency itself may become subject to social or sexual selection because it can convey information about body size and competitive ability (Hall et al., 2013; Linhart & Fuchs, 2015; Brumm & Goymann, 2017). Hence, lower-frequency songs can influence intrasexual competition and mate choice in some species (Beani & Dessì-Fulgheri, 1995; Hardouin et al., 2009; Geberzahn et al., 2010). Morphological variation and signal evolution could therefore become coupled: environmental conditions influence morphology, morphology constrains vocal production, and the resulting geographic variation in song may subsequently interact with sexual and social selection.

Parallelism across islands despite geographic isolation

The consistency of the environmental slopes across Tenerife, La Palma, and Madeira provides an additional biogeographical dimension to these findings. Berthelot's pipit is particularly informative in this respect because its island populations have experienced restricted gene flow, providing opportunities for population-specific divergence (Illera et al., 2007; Spurgin et al., 2014; Armstrong et al., 2018; Martin et al., 2021). Previous work has documented geographically structured song variation in the species, although individual distinctiveness is much stronger than the geographic component of song differentiation (Oñate-Casado et al., 2026). Against this background, the absence of detectable island × environment interactions for song frequency and the multivariate body-size score is notable. The three island populations in our study can be regarded as eco-evolutionary replicates, and the parallelism in the discovered song clines indicates that the elevational pattern is not specific to a single population or island. Indeed, our findings suggest that similar environmental gradients are associated with similar phenotypic responses despite occurring in geographically separated populations.

The contrasting response of body mass, however, indicates that this parallelism is not complete. Whereas wing and head length showed broadly consistent relationships with elevation across islands, body mass responded differently, with Madeira accounting for the clearest positive relationship. This heterogeneity suggests that local ecological conditions can modify components of the response even when broader structural and acoustic patterns remain similar. Such population-specific effects are consistent with the idea that geographic phenotypes emerge from interactions between common environmental constraints and local ecological or evolutionary histories, rather than from a single deterministic response to temperature.

From elevational gradients to macroecology

Taken together, our findings contribute to a broader macroecological perspective in which environmental gradients are viewed not simply as predictors of individual traits, but as potential pathways linking multiple components of phenotype across geographic space. Elevation structures temperature and other environmental variables, which in turn can be associated with variation in morphology and signal characteristics. The resulting phenotypic covariance provides a mechanism by which large-scale ecological and biogeographical patterns can extend into traits that directly mediate interactions between individuals. This perspective complements recent evidence showing that macroecological variation in body size can be reflected in song frequency (Sebastianelli et al., 2022; Hay et al., 2024), while the contrasting elevational patterns reported in other species demonstrate that these relationships are contingent on species-specific ecology and evolutionary history. In Berthelot's pipit, the repeated association of colder, higher environments with larger body size and lower-frequency song across islands suggests that climatic heterogeneity can structure multiple, functionally connected phenotypic dimensions within a species. More broadly, such links may become increasingly important under environmental

change: shifts in temperature and associated changes in body size could alter the acoustic phenotypes of bird songs, potentially coupling climatic effects on organismal morphology with consequences for animal communication and biogeographic differentiation.

ACKNOWLEDGEMENTS: We thank Sailee P. Sakhalkar for providing useful comments that improved the manuscript. The study complied with all relevant national legislation in Spain regarding animal welfare and the protection of wildlife. Birds were captured and ringed by an authorized ringer (Juan Carlos Illera). Permits for capturing, ringing, and bleeding birds were granted by the Regional Government of the Canary Islands (Exp.: 2019/11937) and the Regional Government of Madeira (N. 04/IFCN/2020). Additional permits to work within protected areas were issued by the Cabildo of Tenerife (Exp. AFF 141/19) and the National Park of El Teide (Ref. MDV/amp). Sarah Worsley provided sex information for a few individuals included in the morphological dataset.

Javier Oñate-Casado would like to especially dedicate this manuscript to his mother, who passed away shortly before the conception of this study and who always supported and encouraged him in pursuing a scientific career.

AUTHOR CONTRIBUTIONS: Javier Oñate-Casado and Henrik Brumm conceived the study. Javier Oñate-Casado, Tereza Petrusková, and Adam Petrusek recorded the songs and were responsible for the acoustic data collection. Juan Carlos Illera captured the birds, collected the morphological data, and performed the molecular sexing of the individuals used in this study. Javier Oñate-Casado performed the bioacoustic analyses, analyzed the data, and prepared the tables and figures. Javier Oñate-Casado and Henrik Brumm wrote the original draft. Juan Carlos

Illera, Tereza Petruskova, and Adam Petrusek contributed to the editing of the manuscript and interpretation of the results.

FUNDING: The study was supported by the Czech Science Foundation (project no. 21-04023K), Charles University Grant Agency (project no. 400422), and the Max Planck Society.

CONFLICT OF INTEREST STATEMENT: The authors declare no conflicts of interest.

REFERENCE LIST

Alice Boyle, W., Sandercock, B. K., & Martin, K. (2016). Patterns and drivers of intraspecific variation in avian life history along elevational gradients: A meta-analysis. *Biological Reviews*, *91*(2), 469–482. https://doi.org/10.1111/brv.12180

Armstrong, C., Richardson, D. S., Hipperson, H., Horsburgh, G. J., Küpper, C., Percival-Alwyn, L., Clark, M., Burke, T., & Spurgin, L. G. (2018). Genomic associations with bill length and disease reveal drift and selection across island bird populations. *Evolution Letters*, *2*(1), 22–36. https://doi.org/10.1002/evl3.38

Ashton, K. G. (2002). Patterns of within-species body size variation of birds: Strong evidence for Bergmann's rule. *Global Ecology and Biogeography*, *11*(6), 505–523. https://doi.org/10.1046/j.1466-822X.2002.00313.x

Ashton, K. G., & Feldman, C. R. (2003). BERGMANN's RULE IN NONAVIAN REPTILES: TURTLES FOLLOW IT, LIZARDS AND SNAKES REVERSE IT. *Evolution*, *57*(5), 1151–1163. https://doi.org/10.1111/j.0014-3820.2003.tb00324.x

Bala, R., Kumar, R. S., Gokhale, P., Mohan, D., & Barve, S. (2024). House Sparrows Passer domesticus increase in body size and dorsal feather insulation along a Himalayan elevational

546 gradient. *Journal of Field Ornithology*, *95*(2), art10. https://doi.org/10.5751/JFO-00469-
547 950210
548 Bates, D., Maechler, M., Bolker, B., Walker, S., Ly, A., & Jagan, M. (2003). *lme4: Linear*
549 *Mixed-Effects Models using "Eigen" and S4* (p. 2.0-6) [Data set].
550 https://doi.org/10.32614/CRAN.package.lme4
551 Beani, L., & Dessì-Fulgheri, F. (1995). Mate choice in the grey partridge,: Role of physical and
552 behavioural male traits. *Animal Behaviour*, *49*(2), 347–356.
553 https://doi.org/10.1006/anbe.1995.0047
554 Bergmann, C. (1848). *Ueber die Verhältnisse der Wärmeökonomie der Thiere zu ihrer Größe*.
555 Vandenhoeck und Ruprecht.
556 Blackburn, T. M., & Ruggiero, A. (2001). Latitude, elevation and body mass variation in Andean
557 passerine birds. *Global Ecology and Biogeography*, *10*(3), 245–259.
558 https://doi.org/10.1046/j.1466-822X.2001.00237.x
559 Brumm, H., & Goymann, W. (2017). On the natural history of duetting in White-browed
560 Coucals: Sex- and body-size-dependent differences in a collective vocal display. *Journal of*
561 *Ornithology*, *158*(3), 669–678. https://doi.org/10.1007/s10336-016-1429-0
562 Brumm, H., & Naguib, M. (2009). Chapter 1 Environmental Acoustics and the Evolution of Bird
563 Song. In *Advances in the Study of Behavior* (Vol. 40, pp. 1–33). Elsevier.
564 https://doi.org/10.1016/S0065-3454(09)40001-9
565 Caro, L. M., Caycedo-Rosales, P. C., Bowie, R. C. K., Slabbekoorn, H., & Cadena, C. D. (2013).
566 Ecological speciation along an elevational gradient in a tropical passerine bird? *Journal of*
567 *Evolutionary Biology*, *26*(2), 357–374. https://doi.org/10.1111/jeb.12055

Clauss, M., Dittmann, M. T., Müller, D. W. H., Meloro, C., & Codron, D. (2013). Bergmann′s rule in mammals: A cross-species interspecific pattern. *Oikos*, *122*(10), 1465–1472. https://doi.org/10.1111/j.1600-0706.2013.00463.x

Comin, A., & Brumm, H. (2025). Macroecological variation and subspecies divergence in fiery-necked nightjar songs. *Bioacoustics*, *34*(5), 656–671. https://doi.org/10.1080/09524622.2025.2524427

Cox, D. T. C., Brandt, M. J., Mcgregor, R., Ottosson, U., Stevens, M. C., & Cresswell, W. (2011). Patterns of seasonal and yearly mass variation in West African tropical savannah birds. *Ibis*, *153*(4), 672–683. https://doi.org/10.1111/j.1474-919X.2011.01150.x

Cresswell, W. (1998). Diurnal and seasonal mass variation in blackbirds *Turdus merula*: Consequences for mass-dependent predation risk. *Journal of Animal Ecology*, *67*(1), 78–90. https://doi.org/10.1046/j.1365-2656.1998.00174.x

Freeman, B. G. (2017). Little evidence for Bergmann's rule body size clines in passerines along tropical elevational gradients. *Journal of Biogeography*, *44*(3), 502–510. https://doi.org/10.1111/jbi.12812

Geberzahn, N., Goymann, W., & Ten Cate, C. (2010). Threat signaling in female song—Evidence from playbacks in a sex-role reversed bird species. *Behavioral Ecology*, *21*(6), 1147–1155. https://doi.org/10.1093/beheco/arq122

Gohli, J., & Voje, K. L. (2016). An interspecific assessment of Bergmann's rule in 22 mammalian families. *BMC Evolutionary Biology*, *16*(1), 222. https://doi.org/10.1186/s12862-016-0778-x

Gonzalez-Quevedo, C., Davies, R. G., & Richardson, D. S. (2014). Predictors of malaria infection in a wild bird population: Landscape-level analyses reveal climatic and anthropogenic

591 factors. *Journal of Animal Ecology*, *83*(5), 1091–1102. https://doi.org/10.1111/1365-
592 2656.12214
593 Hall, M. L., Kingma, S. A., & Peters, A. (2013). Male Songbird Indicates Body Size with Low-
594 Pitched Advertising Songs. *PLoS ONE*, *8*(2), e56717.
595 https://doi.org/10.1371/journal.pone.0056717
596 Hardouin, L. A., Bretagnolle, V., Tabel, P., Bavoux, C., Burneleau, G., & Reby, D. (2009).
597 Acoustic cues to reproductive success in male owl hoots. *Animal Behaviour*, *78*(4), 907–913.
598 https://doi.org/10.1016/j.anbehav.2009.07.016
599 Hay, E. M., McGee, M. D., White, C. R., & Chown, S. L. (2024). Body size shapes song in
600 honeyeaters. *Proceedings of the Royal Society B: Biological Sciences*, (291: 20240339).
601 https://doi.org/10.1098/rspb.2024.0339
602 Hijmans, R. J. (2021). *geodata: Access Geographic Data* (p. 0.6-9) [Data set].
603 https://doi.org/10.32614/CRAN.package.geodata
604 Hijmans, R. J., Brown, A., Barbosa, A. M., Cordano, E., & Dyba, K. (2020). *terra: Spatial Data*
605 *Analysis* (p. 1.9-50) [Data set]. https://doi.org/10.32614/CRAN.package.terra
606 Illera, J. C. (2007). *Bisbita Caminero Anthus berthelotii. In: Atlas de las aves nidificantes en el*
607 *archipiélago canario (1997–2003).* (Lorenzo, J. A. (Ed)). General de Conservación de la
608 Naturaleza-Sociedad Española de Ornitología,.
609 Illera, J. C., Emerson, B. C., & Richardson, D. S. (2007). Population history of Berthelot's pipit:
610 Colonization, gene flow and morphological divergence in Macaronesia. *Molecular Ecology*,
611 *16*(21), 4599–4612. https://doi.org/10.1111/j.1365-294X.2007.03543.x
612 Kirschel, A. N. G., Blumstein, D. T., Cohen, R. E., Buermann, W., Smith, T. B., & Slabbekoorn,
613 H. (2009). Birdsong tuned to the environment: Green hylia song varies with elevation, tree

cover, and noise. *Behavioral Ecology*, *20*(5), 1089–1095. https://doi.org/10.1093/beheco/arp101

Körner, C. (2007). The use of 'altitude' in ecological research. *Trends in Ecology & Evolution*, *22*(11), 569–574. https://doi.org/10.1016/j.tree.2007.09.006

Kuznetsova, A., Bruun Brockhoff, P., & Haubo Bojesen Christensen, R. (2013). *lmerTest: Tests in Linear Mixed Effects Models* (p. 3.2-1) [Data set]. https://doi.org/10.32614/CRAN.package.lmerTest

Lachlan, R. F. (2024). *Luscinia: A bioacoustics analysis computer program (Version 2.24.09.12.02)* [Computer software]. http://rflachlan. github.io/Luscinia/

Laiolo, P., & Obeso, J. R. (2017). Life-History Responses to the Altitudinal Gradient. In J. Catalan, J. M. Ninot, & M. M. Aniz (Eds.), *High Mountain Conservation in a Changing World* (Vol. 62, pp. 253–283). Springer International Publishing. https://doi.org/10.1007/978-3-319-55982-7_11

Lenth, R. V., & Piaskowski, J. (2017). *emmeans: Estimated Marginal Means, aka Least-Squares Means* (p. 2.0.4) [Data set]. https://doi.org/10.32614/CRAN.package.emmeans

Linhart, P., & Fuchs, R. (2015). Song pitch indicates body size and correlates with males' response to playback in a songbird. *Animal Behaviour*, *103*, 91–98. https://doi.org/10.1016/j.anbehav.2015.01.038

Martín, A., & Lorenzo, J. A. (2001). *Aves del Archipielago Canario*. Lemus Editor.

Martin, C. A., Armstrong, C., Illera, J. C., Emerson, B. C., Richardson, D. S., & Spurgin, L. G. (2021). Genomic variation, population history and within-archipelago adaptation between island bird populations. *Royal Society Open Science*, *8*(2), rsos.201146, 201146. https://doi.org/10.1098/rsos.201146

637 Meiri, S., & Dayan, T. (2003). On the validity of Bergmann's rule. *Journal of Biogeography*,
638 *30*(3), 331–351. https://doi.org/10.1046/j.1365-2699.2003.00837.x
639 Mikula, P., Valcu, M., Brumm, H., Bulla, M., Forstmeier, W., Petrusková, T., Kempenaers, B.,
640 & Albrecht, T. (2021). A global analysis of song frequency in passerines provides no support
641 for the acoustic adaptation hypothesis but suggests a role for sexual selection. *Ecology Letters*,
642 *24*(3), 477–486. https://doi.org/10.1111/ele.13662
643 Olson, V. A., Davies, R. G., Orme, C. D. L., Thomas, G. H., Meiri, S., Blackburn, T. M., Gaston,
644 K. J., Owens, I. P. F., & Bennett, P. M. (2009). Global biogeography and ecology of body size
645 in birds. *Ecology Letters*, *12*(3), 249–259. https://doi.org/10.1111/j.1461-0248.2009.01281.x
646 Oñate-Casado, J., Porteš, M., Beran, V., Petrusek, A., & Petrusková, T. (2023). Guess who?
647 Evaluating individual acoustic monitoring for males and females of the Tawny Pipit, a
648 migratory passerine bird with a simple song. *Journal of Ornithology*, *164*(4), 845–858.
649 https://doi.org/10.1007/s10336-023-02058-8
650 Oñate-Casado, J., Sakhalkar, S. P., Porteš, M., Beran, V., Pérez-Granados, C., Traba, J., Barrero,
651 A., Petrusek, A., & Petrusková, T. (2026). Individuality obscures geographical song variation
652 in two passerine sister species with contrasting distributions and movement ecology. *Ibis*,
653 *168*(1), 95–116. https://doi.org/10.1111/ibi.13429
654 Pebesma, E. (2016). *sf: Simple Features for R* (p. 1.1-3) [Data set].
655 https://doi.org/10.32614/CRAN.package.sf
656 Podos, J. (2001). *Correlated evolution of morphology and vocal signal structure in Darwin's*
657 *Ænches*.

Prada, S., Menezes De Sequeira, M., Figueira, C., & Da Silva, M. O. (2009). Fog precipitation and rainfall interception in the natural forests of Madeira Island (Portugal). *Agricultural and Forest Meteorology*, *149*(6–7), 1179–1187. https://doi.org/10.1016/j.agrformet.2009.02.010

R Core Team. (2025). *R: A Language and Environment for Statistical Computing*. R Foundation for Statistical Computing. https://www.R-project.org/

Riemer, K., Guralnick, R. P., & White, E. P. (2018). No general relationship between mass and temperature in endothermic species. *eLife*, *7*, e27166. https://doi.org/10.7554/eLife.27166

Rodríguez, R. L., Araya-Salas, M., Gray, D. A., Reichert, M. S., Symes, L. B., Wilkins, M. R., Safran, R. J., & Höbel, G. (2015). How acoustic signals scale with individual body size: Common trends across diverse taxa. *Behavioral Ecology*, *26*(1), 168–177. https://doi.org/10.1093/beheco/aru174

Romano, A., Séchaud, R., & Roulin, A. (2021). Generalized evidence for Bergmann's rule: Body size variation in a cosmopolitan owl genus. *Journal of Biogeography*, *48*(1), 51–63. https://doi.org/10.1111/jbi.13981

Ryan, M. J., & Brenowitz, E. A. (1985). The Role of Body Size, Phylogeny, and Ambient Noise in the Evolution of Bird Song. *The American Naturalist*, *126*(1), 87–100.

Sebastianelli, M., Lukhele, S. M., Nwankwo, E. C., Hadjioannou, L., & Kirschel, A. N. G. (2022). Continent-wide patterns of song variation predicted by classical rules of biogeography. *Ecology Letters*, *25*(11), 2448–2462. https://doi.org/10.1111/ele.14102

Specht, R. (2007). *Avisoft-SASLab Pro ver. 4.5, 5. Sound analysis and synthesis software* [Computer software]. Avisoft Bioacoustics. https://avisoft.com/

679 Spurgin, L. G., Illera, J. C., Jorgensen, T. H., Dawson, D. A., & Richardson, D. S. (2014).
680 Genetic and phenotypic divergence in an island bird: Isolation by distance, by colonization or
681 by adaptation? *Molecular Ecology*, *23*(5), 1028–1039. https://doi.org/10.1111/mec.12672
682 Steinbauer, M. J., Irl, S. D. H., González-Mancebo, J. M., Breiner, F. T., Hernández-Hernández,
683 R., Hopfenmüller, S., Kidane, Y., Jentsch, A., & Beierkuhnlein, C. (2017). Plant invasion and
684 speciation along elevational gradients on the oceanic island La Palma, Canary Islands. *Ecology*
685 *and Evolution*, *7*(2), 771–779. https://doi.org/10.1002/ece3.2640
686 Suthers, R. A., & Zollinger, S. A. (2008). From brain to song: The vocal organ and vocal tract. In
687 *Neuroscience of birdsong* ((eds Zeigler, P.H. & Marler, P, pp. 78–98). Cambridge University
688 Press.
689 Wallschläger, D. (1980). Correlation of song frequency and body weight in passerine birds.
690 *Experientia*, *36*(4), 412–412. https://doi.org/10.1007/BF01975119
691 Warren, B. H., Simberloff, D., Ricklefs, R. E., Aguilée, R., Condamine, F. L., Gravel, D.,
692 Morlon, H., Mouquet, N., Rosindell, J., Casquet, J., Conti, E., Cornuault, J., Fernández-
693 Palacios, J. M., Hengl, T., Norder, S. J., Rijsdijk, K. F., Sanmartín, I., Strasberg, D., Triantis,
694 K. A., … Thébaud, C. (2015). Islands as model systems in ecology and evolution: Prospects
695 fifty years after MacArthur-Wilson. *Ecology Letters*, *18*(2), 200–217.
696 https://doi.org/10.1111/ele.12398
697 Whittaker, R. J., Fernández-Palacios, J. M., Matthews, T. J., Borregaard, M. K., & Triantis, K.
698 A. (2017). Island biogeography: Taking the long view of nature's laboratories. *Science*,
699 *357*(6354), eaam8326. https://doi.org/10.1126/science.aam8326
700 Wickham, H. (2016). *ggplot2: Elegant graphics for data analysis* (p. 4.0.3) [Data set].
701 https://doi.org/10.32614/CRAN.package.ggplot2

Wickham, H. (2021). *httr2: Perform HTTP Requests and Process the Responses* (p. 1.3.0) [Data set]. https://doi.org/10.32614/CRAN.package.httr2

Yang, J., Yang, C., Lin, H., Lees, A. C., & Tobias, J. A. (2025). Elevational constraints on flight efficiency shape global gradients in avian wing morphology. *Current Biology*, *35*(8), 1890-1900.e5. https://doi.org/10.1016/j.cub.2025.02.068

Youngflesh, C., Saracco, J. F., Siegel, R. B., & Tingley, M. W. (2022). Abiotic conditions shape spatial and temporal morphological variation in North American birds. *Nature Ecology & Evolution*, *6*(12), 1860–1870. https://doi.org/10.1038/s41559-022-01893-x

TABLES

Table 1. Summary of acoustic and morphological datasets from the three studied island populations of Berthelot's pipit. Sample sizes refer to individual males included in the respective acoustic and morphological datasets. Sampling years list all years represented in each dataset and island. Elevation ranges are based on SRTM 30-m estimates, and temperature ranges are annual mean temperature (BIO1) at sampled locations.

Island	Acoustic data				Morphology data			
	N	Years	Elevation (m a.s.l.)	Temperature (°C)	N	Years	Elevation (m a.s.l.)	Temperature (°C)
Tenerife	139	2021	7–2303	9.4–21.1	74	2005, 2006, 2020	2–2328	9.4–21.1
La Palma	77	2021	23–905	16.2–20.5	29	2006, 2012, 2013	7–2267	11.6–19.3
Madeira	38	2020	64–1775	11.9–19.3	23	2005, 2006	38–1553	12.1–19.3

FIGURE CAPTIONS

Figure 1. Locations and elevations for acoustic and morphological sampling of Berthelot's pipit (*Anthus berthelotii*) on La Palma, Tenerife, and Madeira. The shading indicates elevation above sea level and is shown using the same color scale across all three islands. White contour lines depict 500-m intervals. Blue points indicate acoustic sampling locations and orange points indicate morphological sampling locations. All panels are displayed at the same spatial scale to allow direct comparison of island size and sampling distribution. The islands are shown separately; their arrangement does not represent their relative geographic position or the distance between them. La Palma and Tenerife belong to the Canary Islands (Spain), whereas Madeira belongs to the Madeira Archipelago (Portugal). Figure S1 shows the geographic positions of the three study islands within these archipelagos.

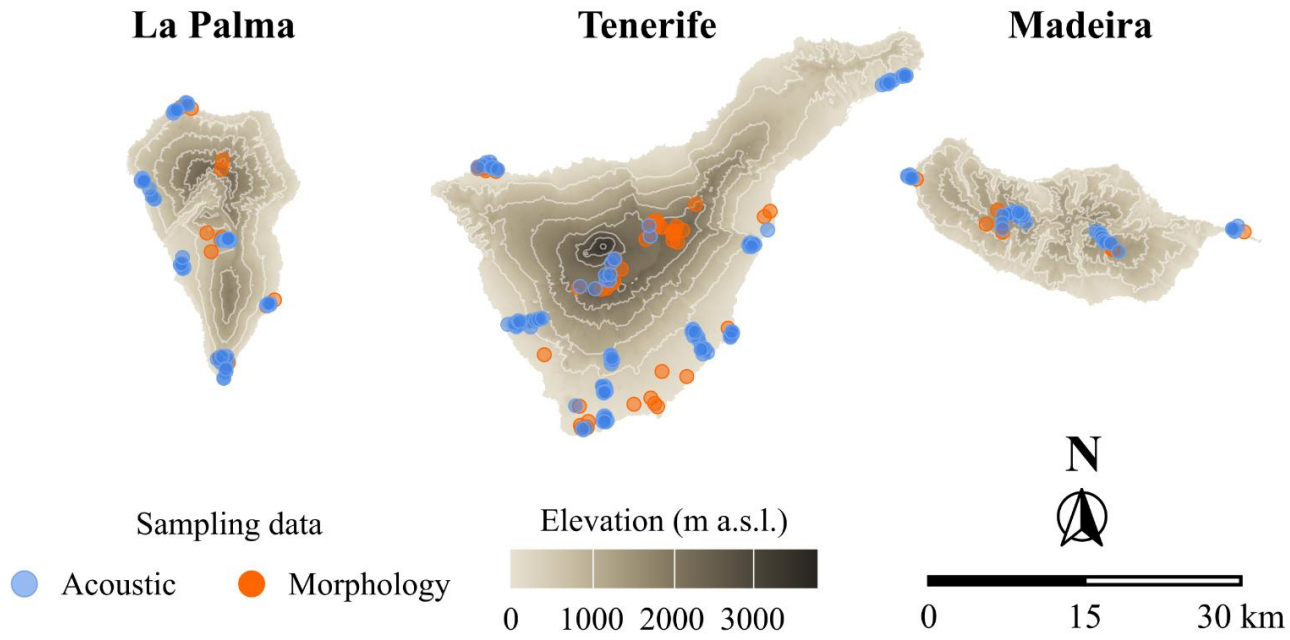
Figure 2. Acoustic frequency variation with elevation across the three island populations of Berthelot's pipit. (A) Song peak frequency and (B) mean element peak frequency in relation to elevation in La Palma, Madeira, and Tenerife. Points denote individual birds (n = 254: La Palma = 77, Madeira = 38, Tenerife = 139) and colors indicate island populations. Lines show model-predicted relationships between elevation and acoustic frequency for each island. Elevation is shown as the environmental gradient because it was strongly correlated with mean annual temperature and yielded the corresponding mirror-image relationships (see Fig. S3A and S3B).

Figure 3. Relationship between the multivariate body-size score and elevation across the three focal islands. Points denote individual birds with complete data for all four traits (n = 125: La Palma = 29, Madeira = 22, Tenerife = 74) and colors indicate island. Lines show model-predicted relationships between elevation and the multivariate body-size index for each island.

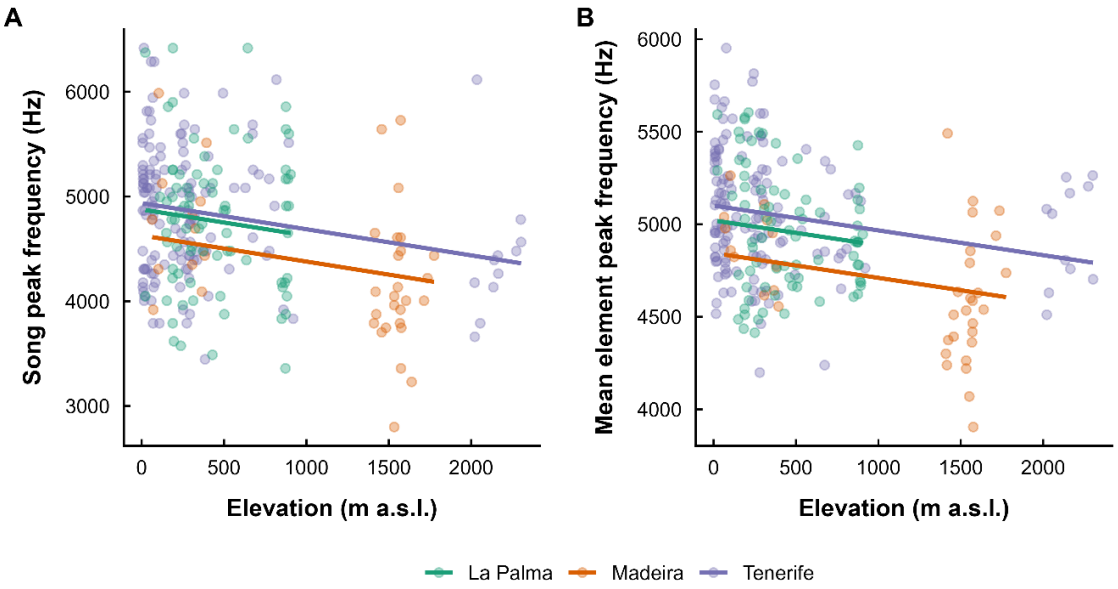
741 Elevation is shown as the environmental gradient because it was strongly correlated with mean
742 annual temperature and yielded the corresponding mirror-image relationships (see Fig. S3C).
743

FIGURES

Figure 1

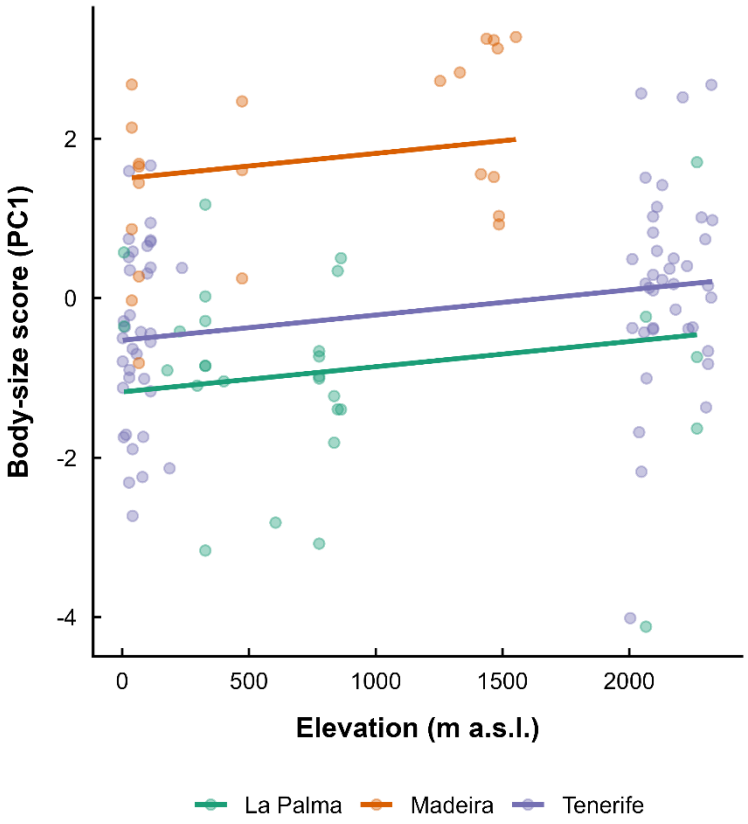


748 Figure 2



749
750

751 Figure 3



752

SUPPLEMENTARY MATERIAL

Title: Elevation gradients shape morphology and acoustic phenotype across isolated songbird populations

Authors: Javier Oñate-Casado, Juan Carlos Illera, Tereza Petrusková, Adam Petrusek, Henrik Brumm

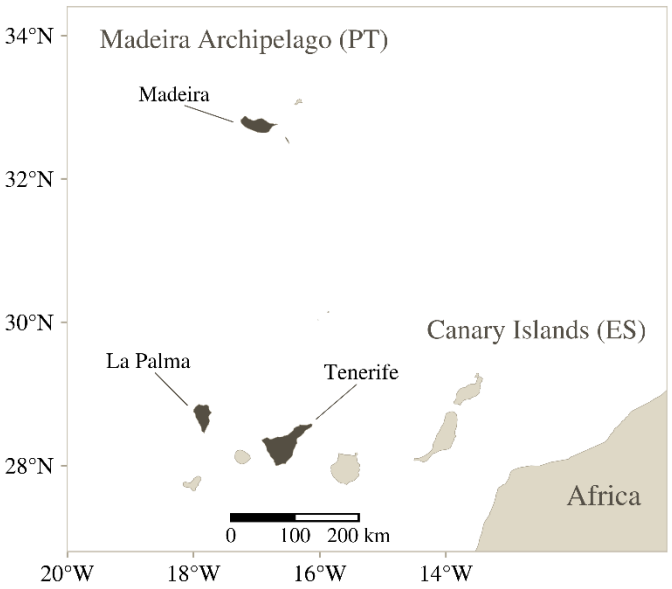


Figure S1. Geographic positions of the three study islands within the Madeira Archipelago (Portugal) and the Canary Islands (Spain). Madeira, La Palma, and Tenerife are highlighted in dark brown; other islands and the African mainland are shown in light beige

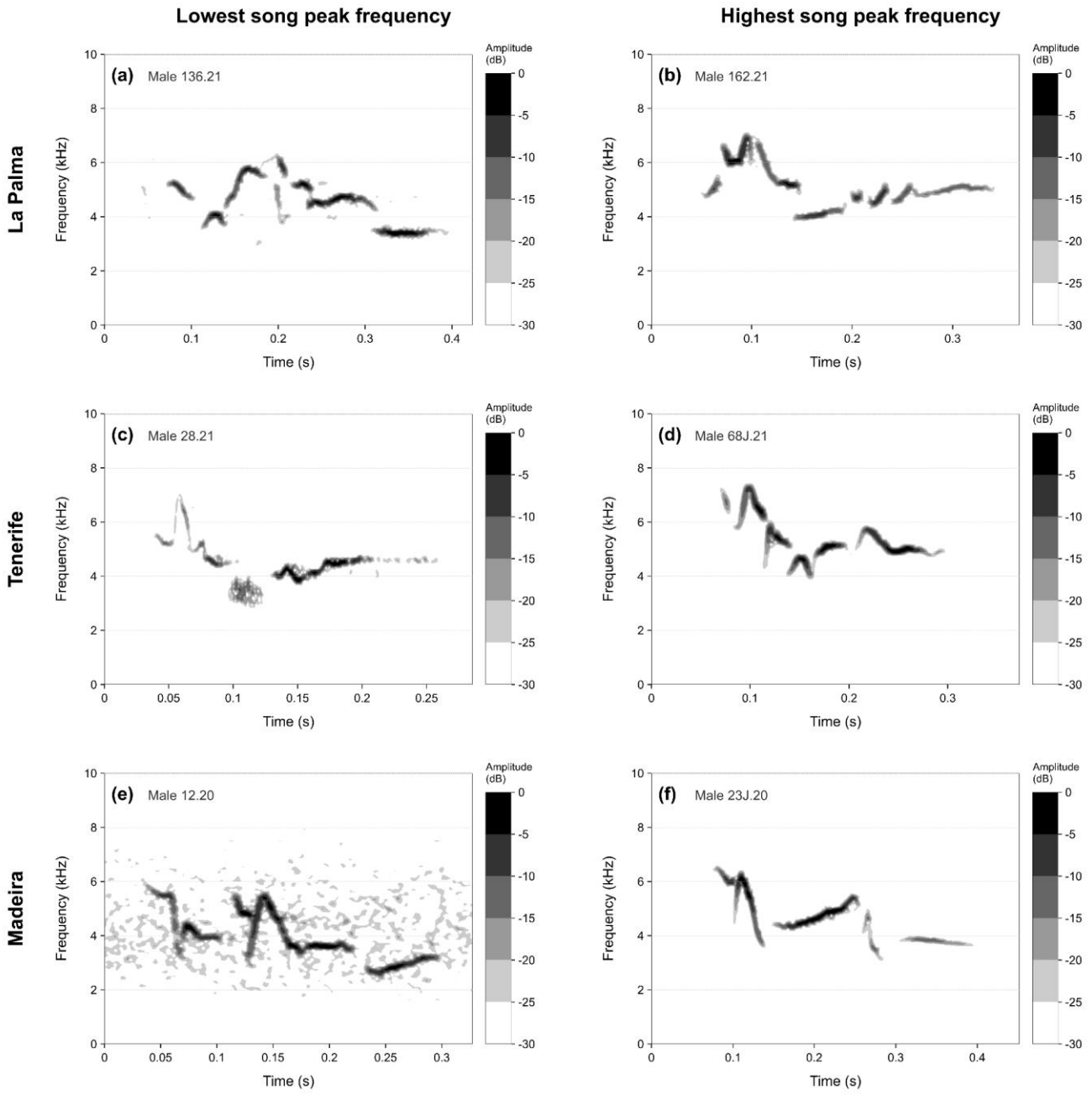


Figure S2. Spectrograms of the Berthelot's pipit songs with the lowest and highest peak frequency recorded on each island: La Palma (a, b), Tenerife (c, d) and Madeira (e, f) (Portugal). The left column (a, c, e) shows the song with the lowest peak frequency on each island (males 136.21, 28.21 and 12.20, respectively). The right column (b, d, f) shows the song with the highest peak frequency (males 162.21, 68J.21 and 23J.20, respectively). Amplitude is shown in greyscale (dB, relative to the maximum amplitude; see color bar), with darker shades indicating higher amplitude. Note that the time axis differs between panels, reflecting differences in song duration.

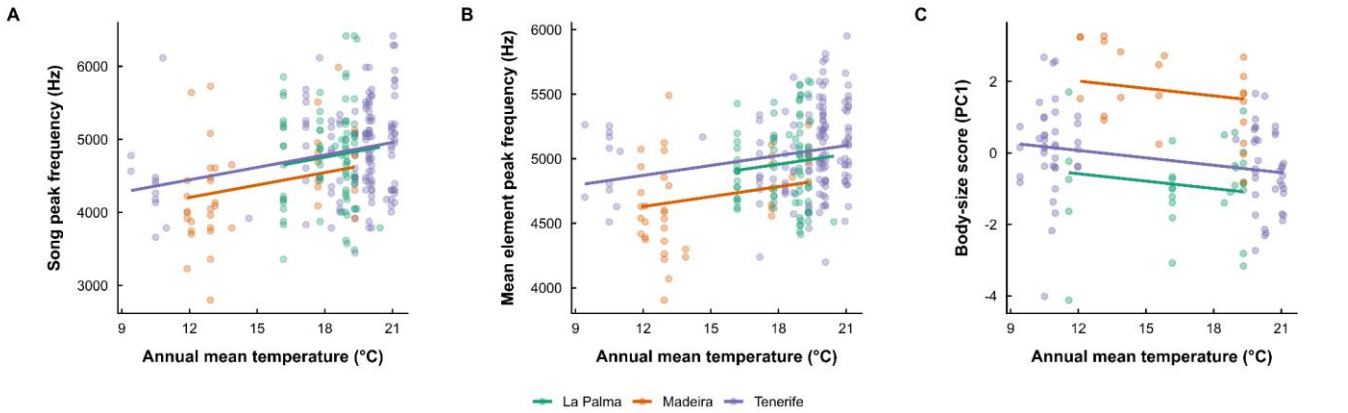


Figure S3. Relationships between annual mean temperature and acoustic and multivariate body-size traits across the three focal islands. (A) Song peak frequency, (B) mean element peak frequency, and (C) multivariate body-size score (PC1) in relation to annual mean temperature (BIO1) in La Palma, Madeira, and Tenerife. In the acoustic panels (A,B), points denote individual birds (n = 254: La Palma = 77, Madeira = 38, Tenerife = 139). In the body-size panel (C), points denote individuals with complete data for all four morphological traits included in the PCA (n = 125: La Palma = 29, Madeira = 22, Tenerife = 74). Colors indicate island populations. Lines show model-predicted relationships between annual mean temperature and each response variable for each island, restricted to the observed temperature range sampled on that island.

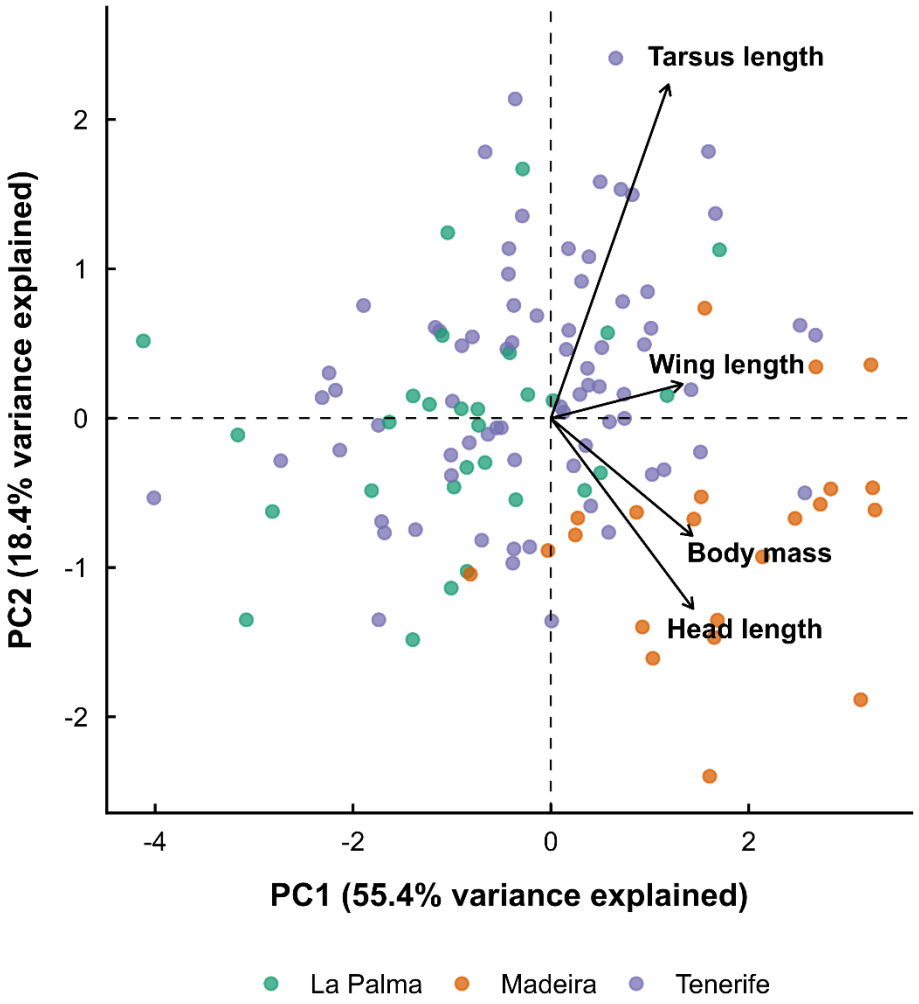


Figure S4. Principal component analysis (PCA) of morphological variation across the three focal islands, based on standardized wing length, head length, tarsus, and body mass. Points represent individual males with complete data for all four traits (n = 125; La Palma = 29, Madeira = 22, Tenerife = 74) and colors indicate islands. Arrows indicate the contribution of each morphological trait to the first two principal components.

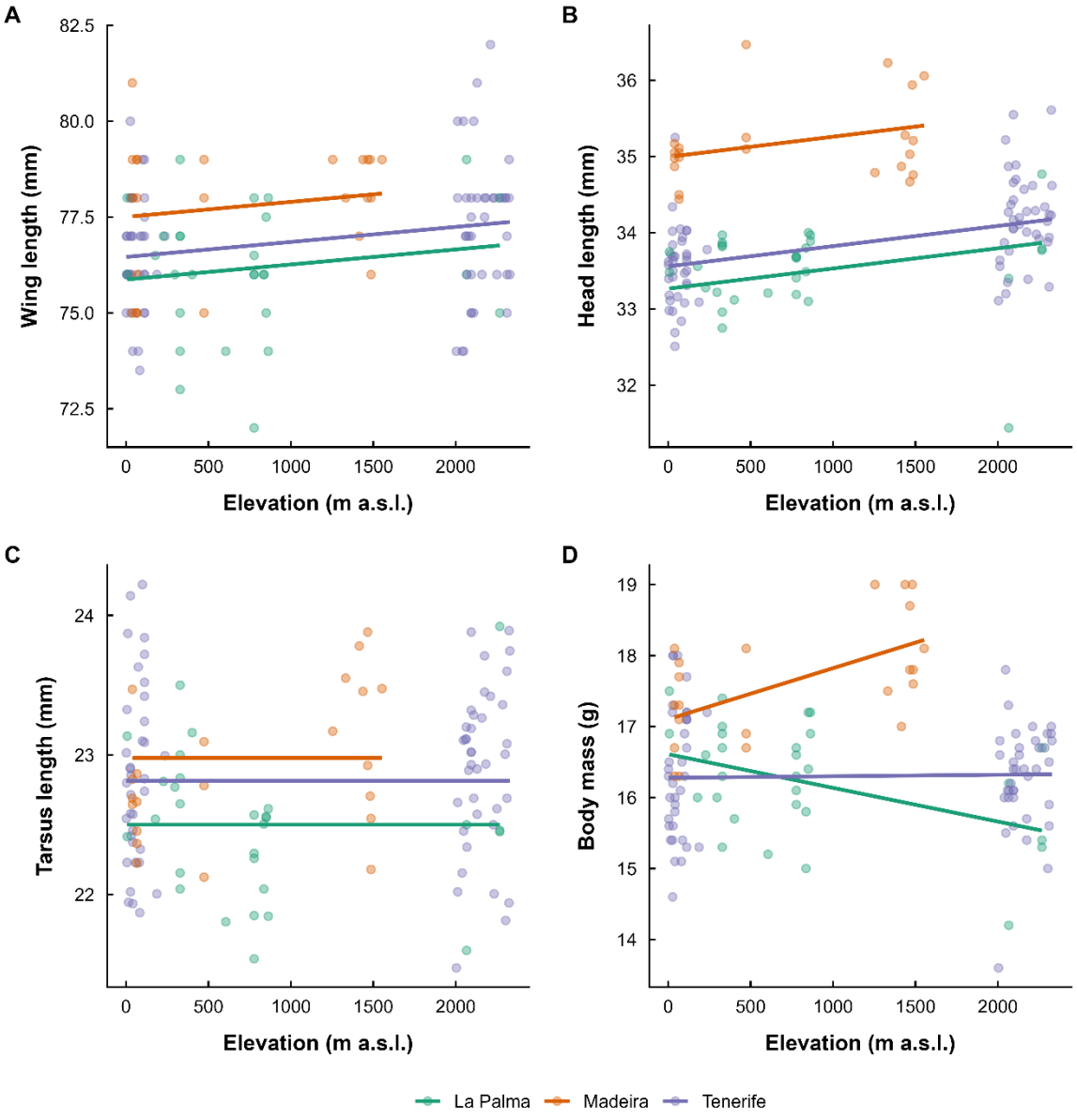


Figure S5. Trait-specific morphological variation with elevation across the three islands. Relationships between elevation and (A) wing length, (B) head length, (C) tarsus length, and (D) body mass in La Palma, Madeira, and Tenerife. Points denote individual birds (A: n = 126; B-D: n = 125), and colors indicate the islands. Lines show model-predicted relationships from the preferred model for each trait: common elevational slopes across islands for wing and head length, no supported elevational relationship for tarsus length, and island-specific elevational slopes for body mass

Table S1. Individual-level acoustic data for male Berthelot's pipits included in the acoustic analyses. Song peak frequency and mean element peak frequency are reported together with recording year, sampling locality, geographic coordinates, SRTM 30-m elevation and annual mean temperature (BIO1) for each individual.

Male ID	Island population	Locality	Song peak frequency (Hz)	Mean element peak frequency (Hz)	Recording year	Latitude	Longitude	Elevation (m a.s.l.)	Annual mean temperature (°C)
03.21 AbTE	Tenerife	Aldea Blanca	5,038.770	4,701.416	2,021	28.06789	-16.63662	245	20.079834
03J.21 AbTE	Tenerife	Aldea Blanca	4,134.375	4,984.937	2,021	28.06769	-16.63405	234	20.079834
05.21 AbTE	Tenerife	Aldea Blanca	5,598.633	5,239.746	2,021	28.06810	-16.63655	243	20.079834
05J.21 AbTE	Tenerife	Aldea Blanca	4,651.172	4,642.559	2,021	28.06747	-16.63544	241	20.079834
07.21 AbTE	Tenerife	Aldea Blanca	4,392.773	4,834.204	2,021	28.06909	-16.63693	242	20.079834
08J.21 AbTE	Tenerife	Aldea Blanca	4,220.508	4,830.615	2,021	28.06315	-16.63331	288	20.079834
10BJ.21 AbTE	Tenerife	Aldea Blanca	4,565.039	4,786.523	2,021	28.06234	-16.63565	295	20.079834
10CJ.21 AbTE	Tenerife	Aldea Blanca	4,737.305	4,633.945	2,021	28.06211	-16.63567	289	20.079834
10J.21 AbTE	Tenerife	Aldea Blanca	4,435.840	5,167.969	2,021	28.06225	-16.63570	292	20.079834
11.21 AbTE	Tenerife	Aldea Blanca	4,866.504	5,598.633	2,021	28.06931	-16.63924	283	20.079834
12J.21 AbTE	Tenerife	Aldea Blanca	3,789.844	5,033.984	2,021	28.06135	-16.63789	274	20.079834
14BJ.21 AbTE	Tenerife	Aldea Blanca	4,306.641	4,938.281	2,021	28.06079	-16.63712	270	20.079834
14J.21 AbTE	Tenerife	Aldea Blanca	5,297.168	5,260.254	2,021	28.06075	-16.63700	268	20.079834
15.21 AbTE	Tenerife	Aldea Blanca	4,306.641	4,198.975	2,021	28.07057	-16.63982	280	20.079834
19.21 AbTE	Tenerife	Aldea Blanca	5,684.766	4,823.438	2,021	28.07075	-16.63662	259	20.079834
23.21 AbTE	Tenerife	Aldea Blanca	5,254.102	5,813.965	2,021	28.06974	-16.63510	244	20.079834
27.21 AbTE	Tenerife	Aldea Blanca	5,598.633	5,770.898	2,021	28.06752	-16.63458	236	20.079834
68J.21 AbTE	Tenerife	El Fraile	6,416.895	5,368.945	2,021	28.00685	-16.66960	14	21.031158
82.21 AbTE	Tenerife	El Fraile	4,134.375	5,103.369	2,021	28.00969	-16.66582	8	21.099167
85.21 AbTE	Tenerife	El Fraile	5,167.969	4,797.598	2,021	28.00833	-16.67077	15	21.031158
191.21 AbTE	Tenerife	El Teide	3,789.844	5,057.227	2,021	28.30349	-16.56684	2,055	10.976000
193.21 AbTE	Tenerife	El Teide	4,392.773	5,254.102	2,021	28.28812	-16.56487	2,140	10.498500
195.21 AbTE	Tenerife	El Teide	4,780.371	5,263.672	2,021	28.25441	-16.62271	2,301	9.412333
195B.21 AbTE	Tenerife	El Teide	4,565.039	4,702.852	2,021	28.25453	-16.62263	2,303	9.412333
196.21 AbTE	Tenerife	El Teide	4,435.840	5,167.969	2,021	28.23191	-16.62922	2,162	10.499001
198.21 AbTE	Tenerife	El Teide	4,134.375	4,806.211	2,021	28.22322	-16.63040	2,135	10.499001
200.21 AbTE	Tenerife	El Teide	4,263.574	4,758.838	2,021	28.23148	-16.63709	2,165	10.499001

Male ID	Island population	Locality	Song peak frequency (Hz)	Mean element peak frequency (Hz)	Recording year	Latitude	Longitude	Elevation (m a.s.l.)	Annual mean temperature (°C)
203.21 AbTE	Tenerife	El Teide	4,177.441	5,081.836	2,021	28.22492	-16.63588	2,021	10.499001
204.21 AbTE	Tenerife	El Teide	3,660.645	4,511.206	2,021	28.21114	-16.65343	2,022	10.499001
205.21 AbTE	Tenerife	El Teide	6,115.430	4,629.639	2,021	28.21431	-16.67827	2,035	10.824500
206.21 AbTE	Tenerife	El Teide	4,478.906	5,204.883	2,021	28.24910	-16.62739	2,274	10.499001
55J.21 AbTE	Tenerife	Guargacho	4,392.773	5,243.335	2,021	28.02220	-16.63824	61	21.099167
56J.21 AbTE	Tenerife	Guargacho	5,727.832	5,569.922	2,021	28.02454	-16.63763	57	21.099167
57.21 AbTE	Tenerife	Guargacho	6,287.695	5,455.078	2,021	28.01958	-16.63779	58	21.099167
58.21 AbTE	Tenerife	Guargacho	5,081.836	5,217.188	2,021	28.01895	-16.63659	49	21.099167
58J.21 AbTE	Tenerife	Guargacho	4,263.574	4,629.639	2,021	28.02758	-16.63570	61	21.099167
59.21 AbTE	Tenerife	Guargacho	5,813.965	5,167.969	2,021	28.01937	-16.63537	47	21.099167
59B.21 AbTE	Tenerife	Guargacho	5,598.633	5,114.136	2,021	28.01924	-16.63535	46	21.099167
59J.21 AbTE	Tenerife	Guargacho	5,943.164	5,157.202	2,021	28.02618	-16.63359	68	21.099167
60.21 AbTE	Tenerife	Guargacho	5,813.965	5,407.227	2,021	28.01914	-16.63258	32	21.099167
60B.21 AbTE	Tenerife	Guargacho	4,306.641	5,401.758	2,021	28.01914	-16.63270	33	21.099167
61.21 AbTE	Tenerife	Guargacho	5,081.836	4,952.637	2,021	28.02048	-16.63092	35	21.099167
62.21 AbTE	Tenerife	Guargacho	5,211.035	4,978.477	2,021	28.02242	-16.63199	50	21.099167
63.21 AbTE	Tenerife	Guargacho	4,952.637	4,860.352	2,021	28.02318	-16.63346	64	21.099167
64.21 AbTE	Tenerife	Guargacho	4,995.703	5,486.660	2,021	28.02267	-16.63603	77	21.099167
18.21 AbTE	Tenerife	La Medida	4,478.906	4,952.637	2,021	28.27520	-16.39871	333	19.345602
20.21 AbTE	Tenerife	La Medida	4,478.906	4,616.719	2,021	28.27583	-16.40173	392	19.345602
22.21 AbTE	Tenerife	La Medida	5,081.836	5,340.234	2,021	28.27705	-16.40354	417	19.345602
22B.21 AbTE	Tenerife	La Medida	4,608.105	4,909.570	2,021	28.27704	-16.40368	420	19.345602
24.21 AbTE	Tenerife	La Medida	4,048.242	4,900.957	2,021	28.27943	-16.40251	405	19.345602
24B.21 AbTE	Tenerife	La Medida	5,383.301	5,030.939	2,021	28.27942	-16.40246	405	19.345602
28.21 AbTE	Tenerife	La Medida	3,445.312	5,012.930	2,021	28.28063	-16.40111	385	19.345602
29.21 AbTE	Tenerife	La Medida	5,038.770	5,090.449	2,021	28.27950	-16.40145	389	19.345602
30J.21 AbTE	Tenerife	La Medida	4,392.773	4,572.217	2,021	28.27480	-16.39910	336	19.345602
31J.21 AbTE	Tenerife	La Medida	4,478.906	4,780.371	2,021	28.27460	-16.40248	379	19.345602
32.21 AbTE	Tenerife	La Medida	4,435.840	4,461.680	2,021	28.27889	-16.39542	287	19.345602
32B.21 AbTE	Tenerife	La Medida	5,081.836	5,476.611	2,021	28.27879	-16.39535	286	19.345602

Male ID	Island population	Locality	Song peak frequency (Hz)	Mean element peak frequency (Hz)	Recording year	Latitude	Longitude	Elevation (m a.s.l.)	Annual mean temperature (°C)
35BJ.21 AbTE	Tenerife	La Medida	4,780.371	5,291.016	2,021	28.27880	-16.39699	321	19.345602
35J.21 AbTE	Tenerife	La Medida	4,823.438	4,640.405	2,021	28.27874	-16.39706	321	19.345602
37J.21 AbTE	Tenerife	La Medida	3,919.043	4,586.572	2,021	28.27775	-16.39365	252	19.345602
70J.21 AbTE	Tenerife	Los Silos-Buenavista	5,555.566	5,753.672	2,021	28.38472	-16.82211	7	19.970833
72J.21 AbTE	Tenerife	Los Silos-Buenavista	5,254.102	5,291.016	2,021	28.38651	-16.82488	7	19.970833
73J.21 AbTE	Tenerife	Los Silos-Buenavista	5,297.168	5,361.768	2,021	28.38810	-16.82604	8	19.970833
74J.21 AbTE	Tenerife	Los Silos-Buenavista	5,081.836	4,964.941	2,021	28.39196	-16.82791	9	19.970833
76J.21 AbTE	Tenerife	Los Silos-Buenavista	4,866.504	5,232.568	2,021	28.39117	-16.83420	19	19.850834
77J.21 AbTE	Tenerife	Los Silos-Buenavista	5,081.836	5,167.969	2,021	28.38695	-16.84089	33	19.850834
78J.21 AbTE	Tenerife	Los Silos-Buenavista	5,469.434	5,002.881	2,021	28.38359	-16.84805	48	19.850834
86.21 AbTE	Tenerife	Los Silos-Buenavista	5,512.500	5,334.082	2,021	28.38063	-16.81563	7	19.970833
91.21 AbTE	Tenerife	Los Silos-Buenavista	5,124.902	5,397.656	2,021	28.38412	-16.82360	10	19.970833
92.21 AbTE	Tenerife	Los Silos-Buenavista	4,823.438	4,715.771	2,021	28.38268	-16.82446	28	19.970833
93.21 AbTE	Tenerife	Los Silos-Buenavista	5,038.770	5,340.234	2,021	28.38481	-16.82562	22	19.970833
96.21 AbTE	Tenerife	Los Silos-Buenavista	4,478.906	5,673.999	2,021	28.38147	-16.81579	7	19.970833
171.21 AbTE	Tenerife	Northeast	4,005.176	4,897.266	2,021	28.52417	-16.15130	59	18.669445
171B.21 AbTE	Tenerife	Northeast	5,254.102	5,630.933	2,021	28.52405	-16.15130	50	18.669445
172.21 AbTE	Tenerife	Northeast	5,340.234	5,096.191	2,021	28.52402	-16.14946	75	18.669445
172B.21 AbTE	Tenerife	Northeast	4,435.840	4,737.305	2,021	28.52411	-16.14940	81	18.669445
173.21 AbTE	Tenerife	Northeast	5,211.035	5,260.254	2,021	28.52416	-16.14914	87	18.669445
176.21 AbTE	Tenerife	Northeast	4,134.375	4,909.570	2,021	28.52531	-16.15166	73	18.669445
178.21. AbTE	Tenerife	Northeast	4,048.242	4,573.652	2,021	28.52316	-16.15569	18	18.669445
179.21 AbTE	Tenerife	Northeast	5,254.102	5,038.770	2,021	28.51757	-16.17505	139	18.295238
180.21 AbTE	Tenerife	Northeast	4,263.574	4,814.824	2,021	28.51411	-16.17668	74	18.295238
181.21 AbTE	Tenerife	Northeast	5,167.969	4,935.410	2,021	28.51720	-16.17055	86	18.295238
182.21 AbTE	Tenerife	Northeast	4,823.438	4,792.676	2,021	28.51400	-16.17673	71	18.295238
183.21 AbTE	Tenerife	Northeast	4,349.707	4,744.482	2,021	28.51225	-16.17843	139	18.295238
184.21 AbTE	Tenerife	Northeast	5,038.770	5,367.151	2,021	28.51489	-16.18125	172	18.295238
185.21 AbTE	Tenerife	Northeast	4,866.504	4,758.838	2,021	28.51058	-16.18831	72	18.295238
190.21 AbTE	Tenerife	Northeast	3,789.844	4,728.691	2,021	28.51217	-16.18241	70	18.295238

Male ID	Island population	Locality	Song peak frequency (Hz)	Mean element peak frequency (Hz)	Recording year	Latitude	Longitude	Elevation (m a.s.l.)	Annual mean temperature (°C)
28J.21 AbTE	Tenerife	Puertito de Güímar	4,306.641	4,801.904	2,021	28.29925	-16.37295	21	21.056250
33.21 AbTE	Tenerife	Punta de Abona	4,306.641	4,823.438	2,021	28.15057	-16.42867	12	20.948717
34.21 AbTE	Tenerife	Punta de Abona	4,091.309	4,873.682	2,021	28.15107	-16.42844	11	20.948717
36.21 AbTE	Tenerife	Punta de Abona	4,005.176	4,516.589	2,021	28.14843	-16.42831	15	20.948717
37.21 AbTE	Tenerife	Punta de Abona	4,866.504	4,952.637	2,021	28.14769	-16.42910	8	20.948717
38J.21 AbTE	Tenerife	Punta de Abona	5,124.902	4,952.637	2,021	28.15164	-16.42965	12	20.948717
40.21 AbTE	Tenerife	Punta de Abona	5,211.035	5,440.723	2,021	28.14718	-16.43053	9	20.948717
40B.21 AbTE	Tenerife	Punta de Abona	4,306.641	5,001.086	2,021	28.14871	-16.43155	18	20.948717
40J.21 AbTE	Tenerife	Punta de Abona	5,038.770	5,129.688	2,021	28.14736	-16.43238	14	20.948717
42BJ.21 AbTE	Tenerife	Punta de Abona	4,177.441	4,823.438	2,021	28.14370	-16.43175	9	20.948717
42J.21 AbTE	Tenerife	Punta de Abona	5,167.969	5,383.301	2,021	28.14372	-16.43189	9	20.948717
16J.21 AbTE	Tenerife	San Miguel de Abona	3,832.910	4,763.145	2,021	28.11562	-16.62669	920	17.170668
18J.21 AbTE	Tenerife	San Miguel de Abona	5,512.500	5,124.902	2,021	28.11425	-16.62726	893	17.170668
20J.21 AbTE	Tenerife	San Miguel de Abona	6,115.430	5,160.791	2,021	28.11167	-16.62458	818	17.767834
22J.21 AbTE	Tenerife	San Miguel de Abona	4,909.570	4,866.504	2,021	28.10965	-16.62638	807	17.170668
25J.21 AbTE	Tenerife	San Miguel de Abona	4,478.906	4,841.895	2,021	28.10799	-16.62340	775	17.767834
27J.21 AbTE	Tenerife	San Miguel de Abona	5,598.633	4,238.965	2,021	28.10270	-16.62558	674	17.170668
43.21 AbTE	Tenerife	San Miguel de Tajao	6,287.695	5,951.777	2,021	28.04161	-16.68275	77	21.031158
43J.21 AbTE	Tenerife	San Miguel de Tajao	3,875.977	4,926.797	2,021	28.15220	-16.49494	293	19.967501
44.21 AbTE	Tenerife	San Miguel de Tajao	4,909.570	5,663.232	2,021	28.11867	-16.47615	66	20.968889
44J.21 AbTE	Tenerife	San Miguel de Tajao	5,124.902	5,443.594	2,021	28.15201	-16.49423	301	19.967501
45J.21 AbTE	Tenerife	San Miguel de Tajao	4,392.773	4,809.082	2,021	28.15345	-16.49262	317	19.967501
46.21 AbTE	Tenerife	San Miguel de Tajao	5,469.434	5,569.922	2,021	28.12521	-16.47919	115	19.967501
46B.21 AbTE	Tenerife	San Miguel de Tajao	5,383.301	4,995.703	2,021	28.12520	-16.47925	115	19.967501
47.21 AbTE	Tenerife	San Miguel de Tajao	4,565.039	5,225.391	2,021	28.14447	-16.49186	258	19.967501
49.21 AbTE	Tenerife	San Miguel de Tajao	4,737.305	5,297.168	2,021	28.15050	-16.49490	295	19.967501
51.21 AbTE	Tenerife	San Miguel de Tajao	5,641.699	5,221.802	2,021	28.15457	-16.49329	323	19.967501
52.21 AbTE	Tenerife	San Miguel de Tajao	4,780.371	5,130.286	2,021	28.15042	-16.48970	300	19.967501
52J.21 AbTE	Tenerife	San Miguel de Tajao	5,081.836	5,223.340	2,021	28.12599	-16.47252	92	19.967501
54.21 AbTE	Tenerife	San Miguel de Tajao	5,986.230	5,030.156	2,021	28.14325	-16.48475	258	19.967501

Male ID	Island population	Locality	Song peak frequency (Hz)	Mean element peak frequency (Hz)	Recording year	Latitude	Longitude	Elevation (m a.s.l.)	Annual mean temperature (°C)
54J.21 AbTE	Tenerife	San Miguel de Tajao	4,780.371	5,114.136	2,021	28.12121	-16.46887	66	20.968889
55.21 AbTE	Tenerife	San Miguel de Tajao	4,694.238	5,474.817	2,021	28.13848	-16.48323	205	19.967501
56.21 AbTE	Tenerife	San Miguel de Tajao	3,789.844	4,633.945	2,021	28.12710	-16.47551	108	19.967501
56B.21 AbTE	Tenerife	San Miguel de Tajao	4,737.305	5,189.502	2,021	28.12716	-16.47558	109	19.967501
61J.21 AbTE	Tenerife	Tijoco	5,081.836	4,839.587	2,021	28.16378	-16.75249	630	19.820486
62J.21 AbTE	Tenerife	Tijoco	5,211.035	5,297.168	2,021	28.16491	-16.74776	711	17.159666
65J.21 AbTE	Tenerife	Tijoco	5,986.230	4,726.538	2,021	28.15443	-16.75792	494	19.820486
66.21 AbTE	Tenerife	Tijoco	4,306.641	4,966.992	2,021	28.16320	-16.75802	532	19.820486
66J.21 AbTE	Tenerife	Tijoco	4,478.906	4,583.496	2,021	28.15451	-16.78109	232	19.820486
67.21 AbTE	Tenerife	Tijoco	5,081.836	5,404.834	2,021	28.16380	-16.75666	562	19.820486
69.21 AbTE	Tenerife	Tijoco	4,608.105	4,852.148	2,021	28.16470	-16.74992	675	17.159666
69B.21 AbTE	Tenerife	Tijoco	5,254.102	5,340.234	2,021	28.16471	-16.74977	677	17.159666
69C.21 AbTE	Tenerife	Tijoco	5,684.766	5,038.770	2,021	28.16460	-16.74997	674	17.159666
70.21 AbTE	Tenerife	Tijoco	5,167.969	4,651.172	2,021	28.16612	-16.74448	774	17.159666
71.21 AbTE	Tenerife	Tijoco	4,435.840	4,817.285	2,021	28.16535	-16.74528	759	17.159666
74.21 AbTE	Tenerife	Tijoco	3,919.043	5,167.969	2,021	28.16732	-16.73913	861	14.641334
76.21 AbTE	Tenerife	Tijoco	4,995.703	5,598.633	2,021	28.15807	-16.77471	304	19.820486
77.21 AbTE	Tenerife	Tijoco	5,512.500	4,921.875	2,021	28.15576	-16.77996	250	19.820486
78.21 AbTE	Tenerife	Tijoco	4,177.441	4,983.398	2,021	28.15776	-16.79508	83	20.737499
79.21 AbTE	Tenerife	Tijoco	4,435.840	4,978.477	2,021	28.15935	-16.78531	192	19.820486
80.21 AbTE	Tenerife	Tijoco	5,426.367	5,182.324	2,021	28.16314	-16.77837	254	19.820486
81.21 AbTE	Tenerife	Tijoco	5,038.770	5,480.200	2,021	28.16241	-16.77582	288	19.820486
106J.21 AbLP	La Palma	El Palmar	5,081.836	5,496.350	2,021	28.83922	-17.93478	275	18.983929
107J.21 AbLP	La Palma	El Palmar	3,962.109	4,414.307	2,021	28.84031	-17.93173	250	18.983929
141.21 AbLP	La Palma	El Palmar	4,694.238	5,014.160	2,021	28.83657	-17.93569	348	18.983929
142.21 AbLP	La Palma	El Palmar	4,177.441	5,490.967	2,021	28.83883	-17.93372	297	18.983929
143.21 AbLP	La Palma	El Palmar	4,478.906	4,521.973	2,021	28.83873	-17.93374	299	18.983929
144.21 AbLP	La Palma	El Palmar	4,694.238	4,485.059	2,021	28.83990	-17.93359	271	18.983929
145.21 AbLP	La Palma	El Palmar	3,574.512	4,875.117	2,021	28.84152	-17.92985	238	18.983929
121.21 AbLP	La Palma	El Paso	4,177.441	4,608.105	2,021	28.65467	-17.85000	850	16.168333

Male ID	Island population	Locality	Song peak frequency (Hz)	Mean element peak frequency (Hz)	Recording year	Latitude	Longitude	Elevation (m a.s.l.)	Annual mean temperature (°C)
122.21 AbLP	La Palma	El Paso	3,832.910	4,828.821	2,021	28.65463	-17.84942	850	16.168333
123.21 AbLP	La Palma	El Paso	4,134.375	4,909.570	2,021	28.65517	-17.84751	856	16.168333
124.21 AbLP	La Palma	El Paso	4,177.441	4,902.393	2,021	28.65471	-17.84598	870	16.168333
126.21 AbLP	La Palma	El Paso	5,641.699	4,622.461	2,021	28.65473	-17.84458	876	16.168333
126B.21 AbLP	La Palma	El Paso	5,857.031	5,426.367	2,021	28.65475	-17.84472	876	16.168333
127.21 AbLP	La Palma	El Paso	4,909.570	4,904.187	2,021	28.65468	-17.84373	878	16.168333
129.21 AbLP	La Palma	El Paso	4,220.508	5,196.680	2,021	28.65468	-17.84189	884	16.168333
130.21 AbLP	La Palma	El Paso	4,651.172	5,081.836	2,021	28.65457	-17.84037	887	16.168333
131.21 AbLP	La Palma	El Paso	5,167.969	4,694.238	2,021	28.65457	-17.83908	889	16.168333
132.21 AbLP	La Palma	El Paso	5,598.633	4,685.625	2,021	28.65458	-17.83797	894	16.168333
132B.21 AbLP	La Palma	El Paso	4,909.570	4,668.398	2,021	28.65461	-17.83804	893	16.168333
133.21 AbLP	La Palma	El Paso	5,211.035	4,945.459	2,021	28.65446	-17.83678	905	16.168333
134.21 AbLP	La Palma	El Paso	4,048.242	4,780.371	2,021	28.65564	-17.83954	882	16.168333
135.21 AbLP	La Palma	El Paso	3,875.977	4,780.371	2,021	28.65693	-17.84040	875	16.168333
135B.21 AbLP	La Palma	El Paso	5,167.969	5,132.080	2,021	28.65696	-17.84046	875	16.168333
135C.21 AbLP	La Palma	El Paso	5,254.102	4,902.393	2,021	28.65688	-17.84032	875	16.168333
136.21 AbLP	La Palma	El Paso	3,359.180	4,991.396	2,021	28.65743	-17.84086	873	16.168333
107.21 AbLP	La Palma	Fuencaliente	6,416.895	4,582.266	2,021	28.48708	-17.84654	644	19.316668
108.21 AbLP	La Palma	Fuencaliente	5,555.566	5,063.379	2,021	28.48704	-17.84558	646	19.316668
109.21 AbLP	La Palma	Fuencaliente	4,048.242	4,667.322	2,021	28.48332	-17.85393	478	19.316668
110.21 AbLP	La Palma	Fuencaliente	4,392.773	4,807.288	2,021	28.48634	-17.84805	636	19.316668
112.21 AbLP	La Palma	Fuencaliente	4,478.906	5,028.003	2,021	28.48735	-17.83848	540	19.316668
114.21 AbLP	La Palma	Fuencaliente	5,038.770	4,774.988	2,021	28.48149	-17.83668	430	19.316668
115.21 AbLP	La Palma	Fuencaliente	5,211.035	5,092.603	2,021	28.47518	-17.84060	336	19.316668
117.21 AbLP	La Palma	Fuencaliente	5,081.836	5,604.016	2,021	28.46937	-17.83935	212	19.316668
117B.21 AbLP	La Palma	Fuencaliente	4,521.973	4,588.530	2,021	28.46943	-17.83943	214	19.316668
118.21 AbLP	La Palma	Fuencaliente	4,952.637	5,499.580	2,021	28.46561	-17.83904	153	19.316668
119.21 AbLP	La Palma	Fuencaliente	4,048.242	5,592.480	2,021	28.45573	-17.84245	23	19.422295
119B.21 AbLP	La Palma	Fuencaliente	6,373.828	5,289.990	2,021	28.45579	-17.84235	23	19.423196
120.21 AbLP	La Palma	Fuencaliente	3,488.379	4,516.589	2,021	28.47847	-17.84818	430	19.316668

Male ID	Island population	Locality	Song peak frequency (Hz)	Mean element peak frequency (Hz)	Recording year	Latitude	Longitude	Elevation (m a.s.l.)	Annual mean temperature (°C)
104.21 AbLP	La Palma	Juan Adalid-El Mudo	4,780.371	4,659.785	2,021	28.84932	-17.91237	201	18.753645
105.21 AbLP	La Palma	Juan Adalid-El Mudo	4,995.703	5,153.613	2,021	28.85232	-17.91540	112	18.753645
106.21 AbLP	La Palma	Juan Adalid-El Mudo	4,005.176	4,726.538	2,021	28.85153	-17.91257	153	18.753645
160.21 AbLP	La Palma	Montaña La Laguna	4,909.570	5,186.426	2,021	28.62863	-17.91460	287	18.470167
161.21 AbLP	La Palma	Montaña La Laguna	4,306.641	5,103.369	2,021	28.56349	-17.77453	190	18.939285
162.21 AbLP	La Palma	Montaña La Laguna	6,416.895	5,028.003	2,021	28.56349	-17.77447	190	18.939285
164.21 AbLP	La Palma	Montaña La Laguna	4,220.508	4,543.506	2,021	28.56345	-17.77013	188	18.939285
151.21 AbLP	La Palma	Montaña de Todoque	4,909.570	4,794.727	2,021	28.61361	-17.91190	260	18.920834
152.21 AbLP	La Palma	Montaña de Todoque	4,005.176	4,659.785	2,021	28.61537	-17.91229	313	18.920834
153.21 AbLP	La Palma	Montaña de Todoque	5,555.566	5,038.770	2,021	28.61590	-17.91466	318	18.920834
155.21 AbLP	La Palma	Montaña de Todoque	4,521.973	5,081.836	2,021	28.61490	-17.91464	306	18.920834
156.21 AbLP	La Palma	Montaña de Todoque	4,995.703	4,926.797	2,021	28.61634	-17.91607	292	18.920834
157.21 AbLP	La Palma	Montaña de Todoque	4,866.504	4,903.418	2,021	28.61268	-17.91391	233	18.920834
158.21 AbLP	La Palma	Montaña de Todoque	3,789.844	4,511.206	2,021	28.61812	-17.91823	189	20.452499
159.21 AbLP	La Palma	Montaña de Todoque	5,211.035	5,450.977	2,021	28.61932	-17.91585	231	18.920834
113J.21 AbLP	La Palma	Montaña del Azufre	5,900.098	5,567.871	2,021	28.56265	-17.77387	189	18.939285
114J.21 AbLP	La Palma	Montaña del Azufre	4,995.703	5,261.279	2,021	28.56191	-17.77340	187	18.939285
116J.21 AbLP	La Palma	Montaña del Azufre	5,254.102	5,577.100	2,021	28.56288	-17.77500	189	18.939285
165.21 AbLP	La Palma	Montaña del Azufre	5,254.102	5,201.465	2,021	28.56350	-17.77438	190	18.939285
166.21 AbLP	La Palma	Montaña del Azufre	3,617.578	5,331.621	2,021	28.56387	-17.77305	196	18.939285
167.21 AbLP	La Palma	Montaña del Azufre	4,263.574	4,748.071	2,021	28.56368	-17.77148	222	18.939285
169.21 AbLP	La Palma	Montaña del Azufre	4,780.371	4,435.840	2,021	28.56347	-17.76966	183	18.939285
170.21 AbLP	La Palma	Montaña del Azufre	4,565.039	5,347.412	2,021	28.56456	-17.76977	156	18.939285
172.21 AbLP	La Palma	Montaña del Azufre	4,651.172	4,486.084	2,021	28.56465	-17.76949	150	18.939285
173.21 AbLP	La Palma	Montaña del Azufre	5,857.031	5,462.256	2,021	28.56518	-17.77201	161	18.939285
138.21 AbLP	La Palma	Tijarafe	4,866.504	5,354.590	2,021	28.71189	-17.96306	510	17.793383
138B.21 AbLP	La Palma	Tijarafe	4,651.172	4,708.594	2,021	28.71187	-17.96290	516	17.793383
139.21 AbLP	La Palma	Tijarafe	4,866.504	4,934.180	2,021	28.71537	-17.96670	498	17.793383
140.21 AbLP	La Palma	Tijarafe	5,641.699	5,132.080	2,021	28.72633	-17.97179	561	17.793383

Male ID	Island population	Locality	Song peak frequency (Hz)	Mean element peak frequency (Hz)	Recording year	Latitude	Longitude	Elevation (m a.s.l.)	Annual mean temperature (°C)
108BJ.21 AbLP	La Palma	Tinizara	4,737.305	5,182.324	2,021	28.73880	-17.98552	367	17.793383
108CJ.21 AbLP	La Palma	Tinizara	4,478.906	4,615.283	2,021	28.73869	-17.98531	373	17.793383
108J.21 AbLP	La Palma	Tinizara	5,383.301	4,761.914	2,021	28.73700	-17.98448	382	17.793383
109J.21 AbLP	La Palma	Tinizara	5,254.102	4,712.695	2,021	28.73689	-17.98244	460	17.793383
110J.21 AbLP	La Palma	Tinizara	4,909.570	4,661.938	2,021	28.73933	-17.98179	507	17.793383
146.21 AbLP	La Palma	Tinizara	5,124.902	5,437.134	2,021	28.73701	-17.98461	378	17.793383
147.21 AbLP	La Palma	Tinizara	4,435.840	4,966.992	2,021	28.74165	-17.98367	459	17.793383
148.21 AbLP	La Palma	Tinizara	5,124.902	5,161.816	2,021	28.73951	-17.98355	432	17.793383
149.21 AbLP	La Palma	Tinizara	3,875.977	4,780.371	2,021	28.73800	-17.98178	502	17.793383
150.21 AbLP	La Palma	Tinizara	4,478.906	5,067.480	2,021	28.73730	-17.98090	522	17.793383
60.20 AbM	Madeira	Pico do Arieiro	4,220.508	5,073.223	2,020	32.73690	-16.93202	1,735	11.901334
61.20 AbM	Madeira	Pico do Arieiro	4,005.176	4,629.639	2,020	32.74019	-16.93865	1,605	11.901334
62.20 AbM	Madeira	Pico do Arieiro	4,435.840	4,737.305	2,020	32.73596	-16.92992	1,775	11.901334
63.20 AbM	Madeira	Pico do Arieiro	4,005.176	4,938.281	2,020	32.73106	-16.92777	1,714	11.901334
64.20 AbM	Madeira	Pico do Arieiro	3,229.980	4,539.199	2,020	32.72594	-16.92493	1,639	11.901334
65.20 AbM	Madeira	Pico do Arieiro	3,919.043	4,418.613	2,020	32.72365	-16.92179	1,571	11.901334
66.20 AbM	Madeira	Pico do Arieiro	4,134.375	4,791.138	2,020	32.72289	-16.91224	1,555	13.139667
66B.20 AbM	Madeira	Pico do Arieiro	4,608.105	4,069.775	2,020	32.72229	-16.91190	1,552	13.139667
67.20 AbM	Madeira	Pico do Arieiro	4,091.309	5,490.967	2,020	32.71090	-16.89883	1,420	13.139667
05.20 AbM	Madeira	Plateau area	5,081.836	4,600.928	2,020	32.75929	-17.06294	1,559	12.934834
05B.20 AbM	Madeira	Plateau area	3,359.180	5,124.902	2,020	32.76183	-17.06817	1,574	12.934834
07.20 AbM	Madeira	Plateau area	4,478.906	4,464.551	2,020	32.75796	-17.07082	1,573	12.934834
08.20 AbM	Madeira	Plateau area	4,608.105	4,586.572	2,020	32.75787	-17.07087	1,572	12.934834
10.20 AbM	Madeira	Plateau area	3,962.109	4,534.277	2,020	32.76554	-17.07800	1,533	12.934834
11.20 AbM	Madeira	Plateau area	4,048.242	4,220.508	2,020	32.76565	-17.07796	1,533	12.934834
12.20 AbM	Madeira	Plateau area	2,799.316	4,263.574	2,020	32.76574	-17.07808	1,533	12.934834
13.20 AbM	Madeira	Plateau area	3,746.777	4,635.022	2,020	32.76331	-17.08411	1,483	12.086333
14.20 AbM	Madeira	Plateau area	3,703.711	4,392.773	2,020	32.76167	-17.08886	1,457	12.086333

Male ID	Island population	Locality	Song peak frequency (Hz)	Mean element peak frequency (Hz)	Recording year	Latitude	Longitude	Elevation (m a.s.l.)	Annual mean temperature (°C)
15.20 AbM	Madeira	Plateau area	5,641.699	4,511.206	2,020	32.76160	-17.08892	1,457	12.086333
16.20 AbM	Madeira	Plateau area	3,875.977	4,374.316	2,020	32.75980	-17.09825	1,424	12.086333
19.20 AbM	Madeira	Plateau area	4,651.172	4,238.965	2,020	32.74902	-17.09832	1,416	13.878333
33.20 AbM	Madeira	Plateau area	5,727.832	5,064.609	2,020	32.75096	-17.05823	1,572	12.934834
34.20 AbM	Madeira	Plateau area	4,435.840	4,855.737	2,020	32.75925	-17.06285	1,558	12.934834
35.20 AbM	Madeira	Plateau area	3,746.777	3,904.688	2,020	32.76298	-17.06591	1,576	12.934834
37.20 AbM	Madeira	Plateau area	3,789.844	4,362.012	2,020	32.76477	-17.07125	1,568	12.934834
41.20 AbM	Madeira	Plateau area	3,789.844	4,300.488	2,020	32.74083	-17.09794	1,410	13.878333
43.20 AbM	Madeira	Ponta Do Pargo	4,349.707	4,616.719	2,020	32.81429	-17.26226	307	17.694792
44.20 AbM	Madeira	Ponta Do Pargo	4,694.238	5,021.543	2,020	32.81400	-17.26146	325	17.694792
45J.20 AbM	Madeira	Ponta Do Pargo	4,823.438	5,107.676	2,020	32.81350	-17.26209	308	17.694792
47.20 AbM	Madeira	Ponta Do Pargo	4,091.309	4,642.559	2,020	32.81582	-17.25799	366	17.694792
51J.20 AbM	Madeira	Ponta Do Pargo	4,952.637	4,952.637	2,020	32.81202	-17.25828	358	17.694792
57.20 AbM	Madeira	Ponta Do Pargo	5,512.500	4,556.426	2,020	32.81108	-17.25381	394	17.694792
58.20 AbM	Madeira	Ponta Do Pargo	4,435.840	4,769.604	2,020	32.81120	-17.25534	383	17.694792
04J.20 AbM	Madeira	Ponta de São Lourenço	3,919.043	4,978.477	2,020	32.74283	-16.70082	71	19.329166
21J.20 AbM	Madeira	Ponta de São Lourenço	4,780.371	5,038.770	2,020	32.74476	-16.70182	64	19.329166
23J.20 AbM	Madeira	Ponta de São Lourenço	5,986.230	4,857.891	2,020	32.75050	-16.69570	104	18.609620
27J.20 AbM	Madeira	Ponta de São Lourenço	4,306.641	5,262.715	2,020	32.74619	-16.70152	102	19.329166
32J.20 AbM	Madeira	Ponta de São Lourenço	5,124.902	4,823.438	2,020	32.74622	-16.70491	125	19.329166

Table S2. Individual-level morphological data for male Berthelot's pipits included in the morphological analyses. Morphological measurements comprise wing length, head length, tarsus length and body mass. Tarsus length is the mean of right and left measurements when both were available, or the available measurement when only one side was measured. Sampling locality, capture year, geographic coordinates, SRTM 30-m elevation and annual mean temperature (BIO1) are also reported for each individual.

Male ID	Island population	Locality	Capture year	Wing length (mm)	Head length (mm)	Tarsus length (mm)	Body mass (g)	Latitude	Longitude	Elevation (m a.s.l.)	Annual mean temperature (°C)
L849888	Tenerife	Adeje	2,006	76.0	33.09	22.005	15.3	28.11484	-16.73498	187	20.262501
L254949	Tenerife	Buenavista	2,005	75.0	33.16	22.230	18.0	28.38234	-16.84768	57	19.850834
L254950	Tenerife	Buenavista	2,005	74.0	32.51	21.935	16.0	28.38474	-16.84749	41	19.850834
L254952	Tenerife	Buenavista	2,005	73.5	33.89	21.870	16.5	28.38309	-16.83663	83	19.850834
L254953	Tenerife	Buenavista	2,005	75.0	33.69	22.420	18.0	28.37861	-16.81820	30	19.970833
L254954	Tenerife	Buenavista	2,005	76.0	33.64	22.855	18.0	28.37861	-16.81820	30	19.970833
4L88991	Tenerife	Buenavista (estercolero)	2,020	79.0	34.03	23.840	17.1	28.37939	-16.83484	112	19.850834
4L88992	Tenerife	Buenavista (estercolero)	2,020	77.5	33.34	23.720	17.1	28.37939	-16.83484	112	19.850834
4L88993	Tenerife	Buenavista (estercolero)	2,020	77.0	33.31	23.420	17.2	28.37939	-16.83484	112	19.850834
4L88994	Tenerife	Buenavista (estercolero)	2,020	78.0	34.03	23.240	17.1	28.37939	-16.83484	112	19.850834
4L88995	Tenerife	Buenavista (estercolero)	2,020	75.0	33.50	22.740	17.2	28.37939	-16.83484	112	19.850834
4L88996	Tenerife	Buenavista (estercolero)	2,020	76.0	33.72	23.520	17.7	28.37939	-16.83484	112	19.850834
4L88997	Tenerife	Buenavista (estercolero)	2,020	76.0	33.64	22.830	15.3	28.37939	-16.83484	112	19.850834
4L88998	Tenerife	Buenavista (estercolero)	2,020	75.0	33.69	23.090	16.7	28.37939	-16.83484	112	19.850834
4L88990	Tenerife	Cruce Izaña	2,020	75.0	34.24	22.690	15.9	28.25503	-16.62178	2,311	9.412333
L849893	Tenerife	El Fraile	2,006	76.0	33.72	21.945	15.4	28.00859	-16.67275	15	21.031158
L849894	Tenerife	El Fraile	2,006	76.0	33.11	23.870	16.0	28.00945	-16.66721	11	21.031158
L849896	Tenerife	El Fraile	2,006	77.0	33.50	22.715	15.6	28.01339	-16.67449	29	21.031158
L849897	Tenerife	El Fraile	2,006	76.0	33.40	22.800	15.7	28.00995	-16.66363	3	21.099167
L849898	Tenerife	El Fraile	2,006	76.0	33.18	22.230	15.6	28.01126	-16.66404	6	21.099167
L849899	Tenerife	El Fraile	2,006	77.0	32.98	23.325	16.5	28.01126	-16.66404	6	21.099167
N117401	Tenerife	El Fraile	2,006	76.0	33.42	22.580	16.2	28.01919	-16.66174	28	21.099167
4L23050	Tenerife	El Médano	2,020	80.0	34.34	22.910	15.4	28.04188	-16.54913	26	20.734333
4L23054	Tenerife	El Médano	2,020	78.0	34.02	22.900	17.2	28.04188	-16.54913	26	20.734333
L707995	Tenerife	El Médano	2,006	77.0	33.94	22.325	15.4	28.05432	-16.56025	87	20.734333
L707996	Tenerife	El Médano	2,006	76.0	32.84	22.230	15.1	28.04494	-16.58774	80	20.315332

Male ID	Island population	Locality	Capture year	Wing length (mm)	Head length (mm)	Tarsus length (mm)	Body mass (g)	Latitude	Longitude	Elevation (m a.s.l.)	Annual mean temperature (°C)
L707998	Tenerife	El Médano (Gasolinera)	2,006	77.0	33.78	22.995	17.2	28.09282	-16.54272	236	18.985332
4L23047	Tenerife	Güimar	2,020	77.0	33.08	24.220	16.9	28.31834	-16.37872	99	19.803333
4L23048	Tenerife	Güimar	2,020	79.0	33.47	23.100	16.3	28.31834	-16.37872	99	19.803333
N117544	Tenerife	Güimar	2,006	77.0	32.69	22.460	15.1	28.32617	-16.36930	41	21.056250
N117545	Tenerife	Güimar	2,006	78.0	33.69	22.375	15.8	28.32617	-16.36930	41	21.056250
L707999	Tenerife	Las Cañadas	2,006	76.0	34.62	23.745	16.8	28.29598	-16.52480	2,328	10.481500
L708000	Tenerife	Las Cañadas	2,006	78.0	34.23	21.940	16.9	28.29486	-16.52967	2,323	10.481500
L849885	Tenerife	Las Cañadas	2,006	78.0	33.88	21.815	15.0	28.29103	-16.52772	2,303	10.881500
L849886	Tenerife	Las Cañadas	2,006	76.0	33.92	22.615	16.7	28.28228	-16.52706	2,250	10.881500
L849887	Tenerife	Las Cañadas	2,006	82.0	34.62	23.420	17.0	28.27992	-16.52000	2,211	10.881500
N117404	Tenerife	Las Cañadas	2,006	80.0	33.56	22.660	16.6	28.21189	-16.63528	2,012	10.499001
N117405	Tenerife	Las Cañadas	2,006	78.0	33.64	22.020	16.8	28.21189	-16.63528	2,012	10.499001
N117406	Tenerife	Las Cañadas	2,006	77.0	34.37	22.890	16.2	28.21794	-16.62865	2,079	10.499001
N117407	Tenerife	Las Cañadas	2,006	74.0	33.11	21.475	13.6	28.21061	-16.64326	2,004	10.499001
N117409	Tenerife	Las Cañadas	2,006	81.0	34.20	22.900	16.7	28.22197	-16.62297	2,130	10.276000
N117410	Tenerife	Las Cañadas	2,006	78.0	34.29	22.500	16.8	28.24003	-16.61100	2,228	10.276000
N117412	Tenerife	Las Cañadas	2,006	75.0	34.89	23.285	16.9	28.30328	-16.56008	2,109	10.976000
N117413	Tenerife	Las Cañadas	2,006	80.0	34.70	22.690	16.4	28.30328	-16.56008	2,109	10.976000
N117414	Tenerife	Las Cañadas	2,006	78.0	33.39	22.935	16.3	28.30308	-16.55353	2,183	10.976000
N117415	Tenerife	Las Cañadas	2,006	78.0	33.98	22.005	16.4	28.30133	-16.54753	2,233	10.976000
N117416	Tenerife	Las Cañadas	2,006	76.0	33.76	22.340	16.1	28.30831	-16.55656	2,068	10.976000
N117417	Tenerife	Las Cañadas	2,006	77.0	34.27	23.200	16.0	28.31064	-16.55417	2,064	10.976000
N117418	Tenerife	Las Cañadas	2,006	78.0	34.87	23.115	17.3	28.31064	-16.55417	2,064	10.976000
N117419	Tenerife	Las Cañadas	2,006	77.0	33.35	23.110	16.1	28.30933	-16.56006	2,059	10.976000
N117421	Tenerife	Las Cañadas	2,006	74.0	33.20	22.455	15.5	28.21257	-16.68129	2,048	10.824500
N117422	Tenerife	Las Cañadas	2,006	78.0	34.15	23.005	16.9	28.25426	-16.62256	2,300	9.412333
N117424	Tenerife	Las Cañadas	2,006	76.0	34.57	23.265	16.4	28.28359	-16.57163	2,159	10.498500
N117426	Tenerife	Las Cañadas	2,006	80.0	35.22	23.105	17.8	28.30301	-16.56638	2,047	10.976000
N117427	Tenerife	Las Cañadas	2,006	74.0	33.87	22.155	16.0	28.30433	-16.56431	2,039	10.976000
N117428	Tenerife	Las Cañadas	2,006	78.0	34.11	22.575	16.6	28.29476	-16.56460	2,130	10.976000

Male ID	Island population	Locality	Capture year	Wing length (mm)	Head length (mm)	Tarsus length (mm)	Body mass (g)	Latitude	Longitude	Elevation (m a.s.l.)	Annual mean temperature (°C)
L707993	Tenerife	Las Galletas	2,006	78.0	35.25	22.575	15.9	28.04652	-16.55399	42	20.734333
N117403	Tenerife	Malpaís de Rasca	2,006	74.0	34.05	23.630	16.1	28.04098	-16.67659	74	21.031158
L849891	Tenerife	Polígono de Granadilla	2,006	77.0	32.97	22.020	14.6	28.08599	-16.50218	27	20.261833
L849892	Tenerife	Polígono de Granadilla	2,006	78.0	33.84	24.140	17.3	28.08599	-16.50218	27	20.261833
N117546	Tenerife	Poris de Abona	2,006	75.0	33.58	23.015	16.3	28.15647	-16.43577	2	20.948717
N117547	Tenerife	Poris de Abona	2,006	77.0	33.62	22.545	16.4	28.15647	-16.43577	2	20.948717
4L23051	Tenerife	Teide	2,020	77.5	35.55	23.020	16.0	28.33507	-16.49129	2,094	11.979667
4L88980	Tenerife	Teide	2,020	75.0	34.17	23.190	16.1	28.33507	-16.49129	2,094	11.979667
4L88982	Tenerife	Teide	2,020	77.0	34.06	23.880	16.5	28.33507	-16.49129	2,094	11.979667
4L88983	Tenerife	Teide	2,020	76.0	34.43	23.020	16.4	28.33507	-16.49129	2,094	11.979667
4L88984	Tenerife	Teide	2,020	75.0	34.05	23.320	16.1	28.33507	-16.49129	2,094	11.979667
4L88985	Tenerife	Teide	2,020	78.0	34.66	22.930	15.6	28.33507	-16.49129	2,094	11.979667
4L23052	Tenerife	Teide (Izaña)	2,020	78.0	34.01	23.710	15.7	28.23466	-16.62968	2,175	10.499001
4L88988	Tenerife	Teide (Teleférico)	2,020	77.0	33.94	23.080	16.5	28.25503	-16.62178	2,311	9.412333
4L88989	Tenerife	Teide (Teleférico)	2,020	76.0	33.29	23.600	15.6	28.25503	-16.62178	2,311	9.412333
4L88986	Tenerife	Teide (corral del niño)	2,020	79.0	35.61	23.890	17.0	28.29738	-16.51138	2,324	10.481500
4L88987	Tenerife	Teide (corral del niño)	2,020	78.0	34.34	23.360	16.7	28.30282	-16.52202	2,285	10.481500
4L89000	Tenerife	Teide (parada)	2,020	77.5	34.28	23.450	15.4	28.23466	-16.62968	2,175	10.499001
N117520	La Palma	El Mudo	2,006	77.0	33.28	22.810	16.6	28.84574	-17.92305	227	18.983929
N117501	La Palma	El Paso (Centro Visitantes)	2,006	76.0	33.80	22.040	15.0	28.65916	-17.85123	836	16.168333
N117502	La Palma	El Paso (Centro Visitantes)	2,006	76.0	33.49	22.505	15.8	28.65916	-17.85123	836	16.168333
N117506	La Palma	El Paso (Centro Visitantes)	2,006	77.5	34.00	22.560	17.2	28.65494	-17.85251	850	16.168333
N117516	La Palma	El Paso (Centro Visitantes). Depósito Agua	2,006	75.0	33.10	22.550	16.4	28.65494	-17.85251	850	16.168333
N117503	La Palma	El Paso (Tacande)	2,006	76.0	33.41	22.570	16.7	28.63789	-17.86790	777	16.168333
N117504	La Palma	El Paso (Tacande)	2,006	76.5	33.67	21.850	16.6	28.63789	-17.86790	777	16.168333
N117505	La Palma	El Paso (Tacande)	2,006	72.0	33.19	21.540	16.1	28.63789	-17.86790	777	16.168333
N117514	La Palma	El Paso (Tacande)	2,006	76.0	33.68	22.295	16.3	28.63789	-17.86790	777	16.168333
N117515	La Palma	El Paso (Tacande)	2,006	78.0	33.69	22.260	15.9	28.63789	-17.86790	777	16.168333
L254993	La Palma	Fuencaliente	2,006	73.0	32.75	22.040	15.3	28.47820	-17.83544	328	19.316668

Male ID	Island population	Locality	Capture year	Wing length (mm)	Head length (mm)	Tarsus length (mm)	Body mass (g)	Latitude	Longitude	Elevation (m a.s.l.)	Annual mean temperature (°C)
L254994	La Palma	Fuencaliente	2,006	77.0	33.84	22.835	16.7	28.47820	-17.83544	328	19.316668
L254998	La Palma	Fuencaliente	2,006	74.0	33.82	22.650	16.9	28.47820	-17.83544	328	19.316668
N117518	La Palma	Juan Adalid	2,006	76.0	33.22	22.770	16.0	28.84409	-17.90618	296	18.753645
2L55105	La Palma	La Salemera	2,013	76.5	33.56	22.540	16.0	28.56145	-17.77511	178	18.939285
L254996	La Palma	Las Solivetas	2,006	77.0	32.96	23.500	16.3	28.47820	-17.83544	328	19.316668
2L53406	La Palma	Lucandia	2,013	79.0	33.40	22.500	16.2	28.77053	-17.85250	2,066	11.579166
2N96564	La Palma	Lucandia	2,012	76.0	31.44	21.600	14.2	28.77053	-17.85250	2,066	11.579166
N117512	La Palma	Punta El Lajio	2,006	78.0	33.75	23.135	16.9	28.57050	-17.76248	7	18.939285
N117513	La Palma	Punta El Lajio	2,006	76.0	33.48	22.415	17.5	28.57050	-17.76248	7	18.939285
1N87665	La Palma	Roque 1	2,012	78.0	34.77	23.920	16.7	28.75749	-17.85461	2,267	11.579166
2L41725	La Palma	Roque 1	2,013	75.0	33.77	22.460	15.3	28.75749	-17.85461	2,267	11.579166
2L41726	La Palma	Roque 1	2,013	78.0	33.79	22.450	15.4	28.75749	-17.85461	2,267	11.579166
N117507	La Palma	Tamarahoya	2,006	78.0	33.97	22.615	17.2	28.66495	-17.87576	863	18.470167
N117508	La Palma	Tamarahoya	2,006	74.0	33.89	21.845	16.9	28.66495	-17.87576	863	18.470167
L254997	La Palma	Volcán de San Antonio (Fuencaliente)	2,006	75.0	33.87	22.155	17.0	28.47820	-17.83544	328	19.316668
L255000	La Palma	Volcán de San Antonio (Fuencaliente)	2,006	79.0	33.97	23.000	17.4	28.47820	-17.83544	328	19.316668
N117509	La Palma	Volcán de San Antonio (Fuencaliente)	2,006	74.0	33.21	21.805	15.2	28.48602	-17.84978	605	19.316668
N117511	La Palma	Volcán de Teneguía	2,006	76.0	33.12	23.160	15.7	28.47857	-17.84001	401	19.316668
Madeira 1	Madeira	Casa Sardina	2,006	78.0	34.87	22.690	16.7	32.74237	-16.68472	38	19.329166
Madeira 2	Madeira	Casa Sardina	2,006	75.0	35.17	22.645	16.3	32.74237	-16.68472	38	19.329166
Madeira 4	Madeira	Casa Sardina	2,006	79.0	35.05	22.825	18.1	32.74237	-16.68472	38	19.329166
Madeira 7	Madeira	Casa Sardina	2,006	81.0	34.98	23.470	17.3	32.74237	-16.68472	38	19.329166
Madeira 15	Madeira	Pico de Arriero	2,006	79.0	35.94	22.705	19.0	32.71356	-16.90947	1,481	13.139667
Madeira 17	Madeira	Pico de Arriero	2,006	79.0	36.06	23.475	18.1	32.72212	-16.91272	1,553	13.139667
Madeira 18	Madeira	Pico de Arriero	2,006	76.0	35.21	22.545	17.6	32.71401	-16.90811	1,486	13.139667

Male ID	Island population	Locality	Capture year	Wing length (mm)	Head length (mm)	Tarsus length (mm)	Body mass (g)	Latitude	Longitude	Elevation (m a.s.l.)	Annual mean temperature (°C)
Madeira 19	Madeira	Pico de Arriero	2,006	78.0	34.76	22.180	17.8	32.71401	-16.90811	1,486	13.139667
Madeira 20	Madeira	Pol de Serra	2,006	77.0	34.87	23.780	17.0	32.74132	-17.09789	1,415	13.878333
Madeira 21	Madeira	Pol de Serra	2,006	78.0	34.67	22.925	17.8	32.75904	-17.08737	1,466	12.086333
Madeira 22	Madeira	Pol de Serra	2,006	78.0	36.23	23.550	17.5	32.73561	-17.09754	1,332	13.878333
Madeira 24	Madeira	Pol de Serra	2,006	79.0	35.28	23.455	19.0	32.76731	-17.10677	1,437	12.086333
Madeira 25	Madeira	Pol de Serra	2,006	79.0	34.79	23.170	19.0	32.74695	-17.12592	1,254	15.814931
Madeira 28	Madeira	Pol de Serra	2,006	79.0	35.03	23.880	18.7	32.75904	-17.08737	1,466	12.086333
A109521	Madeira	Punta San Lorenzo	2,005	75.0				32.74489	-16.70209	66	19.329166
Madeira 10	Madeira	Punta San Lorenzo	2,006	79.0	34.99	22.365	17.9	32.74489	-16.70209	66	19.329166
Madeira 11	Madeira	Punta San Lorenzo	2,006	76.0	34.50	22.665	17.1	32.74489	-16.70209	66	19.329166
Madeira 12	Madeira	Punta San Lorenzo	2,006	79.0	35.11	22.455	17.7	32.74489	-16.70209	66	19.329166
Madeira 13	Madeira	Punta San Lorenzo	2,006	75.0	34.44	22.225	16.3	32.74489	-16.70209	66	19.329166
Madeira 9	Madeira	Punta San Lorenzo	2,006	78.0	35.05	22.865	17.3	32.74489	-16.70209	66	19.329166
Madeira 30	Madeira	Punta do Pargo	2,006	75.0	35.10	22.780	16.7	32.80969	-17.24716	473	15.572570
Madeira 31	Madeira	Punta do Pargo	2,006	79.0	35.25	23.095	18.1	32.80969	-17.24716	473	15.572570
Madeira 32	Madeira	Punta do Pargo	2,006	78.0	36.47	22.125	16.9	32.80969	-17.24716	473	15.572570

Table S3. Linear mixed-effects model outputs showing the effects of elevation and annual mean temperature (BIO1) on song peak frequency and mean element peak frequency across the three focal island populations. Estimates indicate the change in the response per unit change in each environmental predictor. Because population × environment interactions were not supported, these estimates describe a common relationship across the three island populations. P environment is the likelihood-ratio test comparing models with and without the environmental predictor, while P interaction tests whether environmental slopes differ among populations.

Response	Predictor	N	Estimate	SE	95% CI	χ^2 environment	df environment	P environment	χ^2 interaction	df interaction	P interaction
Song peak frequency	Elevation (per 1000 m)	254	-249.384	78.839	-403.904 to -94.863	8.35	1	**0.004**	1.89	2	0.390
Song peak frequency	Annual mean temperature (°C)	254	56.815	16.469	24.538 to 89.093	10.11	1	**0.001**	1.96	2	0.376
Element mean peak frequency	Elevation (per 1000 m)	254	-133.963	45.657	-223.449 to -44.478	7.70	1	**0.006**	2.46	2	0.293
Element mean peak frequency	Annual mean temperature (°C)	254	25.654	9.585	6.867 to 44.440	6.22	1	**0.013**	1.50	2	0.473

Table S4. Locality-level sensitivity analyses of acoustic variation along elevational and thermal gradients. Acoustic measurements were averaged within each of 25 sampling localities, and linear models included island population as a fixed effect. Estimates represent the common environmental slope after accounting for differences among island populations**.**

Response	Predictor	N localities	Estimate	SE	95% CI	df	t	P
Song peak frequency	Elevation (per 1000 m)	25	-239.917	104.245	-456.707 to -23.127	21	-2.30	**0.032**
Song peak frequency	Annual mean temperature (°C)	25	52.095	21.993	6.358 to 97.833	21	2.37	**0.028**
Mean element peak frequency	Elevation (per 1000 m)	25	-112.896	51.521	-220.040 to -5.753	21	-2.19	**0.040**
Mean element peak frequency	Annual mean temperature (°C)	25	23.028	11.029	0.092 to 45.965	21	2.09	**0.049**

Table S5. Linear mixed-effects model outputs showing the effects of elevation and annual mean temperature (BIO1) on the multivariate body-size index (PC1), wing length, head length, tarsus length and body mass across the three focal islands. Estimates indicate the change in the response per unit change in each environmental predictor. For most traits, island × environment interactions were not supported, and the estimates therefore describe a common relationship across islands. For body mass, the interaction was supported, indicating that the environmental relationship differed among islands and should therefore be interpreted using island-specific slopes. P environment is the likelihood-ratio test comparing models with and without the environmental predictor, while P interaction tests whether environmental slopes differ among islands.

Response	Predictor	N	Estimate	SE	95% CI	χ^2 environment	df environment	P environment	χ^2 interaction	df interaction	P interaction
Wing length	Elevation (per 1000 m)	126	0.392	0.161	0.076 to 0.709	5.77	1	**0.016**	0.13	2	0.938
Wing length	Annual mean temperature (°C)	126	-0.086	0.036	-0.156 to -0.016	5.69	1	**0.017**	0.34	2	0.845
Head length	Elevation (per 1000 m)	125	0.265	0.062	0.144 to 0.386	16.19	1	**<0.001**	2.79	2	0.247
Head length	Annual mean temperature (°C)	125	-0.056	0.014	-0.083 to -0.030	15.12	1	**<0.001**	2.39	2	0.302
Tarsus length	Elevation (per 1000 m)	125	0.062	0.063	-0.061 to 0.184	0.96	1	0.328	2.34	2	0.311
Tarsus length	Annual mean temperature (°C)	125	-0.012	0.014	-0.039 to 0.015	0.78	1	0.376	1.99	2	0.370
Body mass	Elevation (per 1000 m)	125	0.037	0.090	-0.139 to 0.214	0.17	1	0.681	9.23	2	**0.010**
Body mass	Annual mean temperature (°C)	125	-0.011	0.020	-0.050 to 0.027	0.33	1	0.564	7.87	2	**0.020**
Multivariate body-size index (PC1)	Elevation (per 1000 m)	125	0.316	0.118	0.085 to 0.548	6.85	1	**0.009**	4.37	2	0.112
Multivariate body-size index (PC1)	Annual mean temperature (°C)	125	-0.069	0.026	-0.120 to -0.018	6.73	1	**0.010**	3.91	2	0.142

Table S6. Island-specific outputs for the relationships of body mass with elevation and annual mean temperature (BIO1). These estimates are reported because island × environment interactions were supported for body mass in the corresponding mixed-effects models.

Environmental_predictor	Island	Estimate	SE	df	95% CI	P
Elevation (per 1000 m)	La Palma	-0.475	0.255	54.28	-0.986 to 0.036	0.068
Elevation (per 1000 m)	Madeira	0.720	0.309	52.13	0.099 to 1.340	**0.024**
Elevation (per 1000 m)	Tenerife	0.021	0.098	85.02	-0.173 to 0.216	0.827
Annual mean temperature (°C)	La Palma	0.114	0.065	54.29	-0.015 to 0.243	0.083
Annual mean temperature (°C)	Madeira	-0.150	0.071	48.15	-0.293 to -0.006	**0.041**
Annual mean temperature (°C)	Tenerife	-0.009	0.021	86.89	-0.051 to 0.033	0.686